NUREG/CR-3925
SAND84-1586
Revision

SWIFT II Self-Teaching Curriculum

Illustrative Problems for the Sandia Waste-Isolation Flow and Transport Model for Fractured Media

Manuscript Completed: July 1986
Date Published: August 1986
Date Revised: January 1987

Prepared by
M. Reeves*, D. S. Ward*, P. A. Davis, E. J. Bonano

Sandia National Laboratories
Albuquerque, NM 87185

*GeoTrans, Inc.

Prepared for
Division of Waste Management
Office of Nuclear Material Safety and Safeguards
U.S. Nuclear Regulatory Commission
Washington, DC 20555
NRC FIN A1158

NRC FORM 335 (7-84) NRCM 1102 3201 3202

U.S. NUCLEAR REGULATORY COMMISSION

BIBLIOGRAPHIC DATA SHEET

SEE INSTRUCTIONS ON THE REVERSE

REPORT NUMBER (Assigned by TIDC, add Vol. No., if any)

NUREG/CR-3925
SAND84-1586
REVISION

2 TITLE AND SUBTITLE

SWIFT II Self-Teaching Curriculum: Illustrative Problems for the Sandia Waste-Isolation Flow and Transport Model for Fractured Media

3 LEAVE BLANK

4 DATE REPORT COMPLETED

MONTH	YEAR
July	1986

5 AUTHOR(S)

M. Reeves, D. S. Ward, P. A. Davis, and E. J. Bonano

6 DATE REPORT ISSUED

MONTH	YEAR
January	1987

7 PERFORMING ORGANIZATION NAME AND MAILING ADDRESS (Include Zip Code)

Sandia National Laboratories
Albuquerque, NM 87185

8 PROJECT/TASK/WORK UNIT NUMBER

9 FIN OR GRANT NUMBER

FIN A-1158

10 SPONSORING ORGANIZATION NAME AND MAILING ADDRESS (Include Zip Code)

Division of Waste Management
Office of Nuclear Material Safety & Safeguards
U.S. Nuclear Regulatory Commission
Washington, D.C. 20555

11 TYPE OF REPORT

Final

PERIOD COVERED (Inclusive dates)

12 SUPPLEMENTARY NOTES

13 ABSTRACT (200 words or less)

Several documents have been written describing SWIFT II, the most current version of the SWIFT (Sandia Waste Isolation Flow and Transport) Model. Reeves et al. [1986a], describes the theory and implementation, and Reeves et al. [1986b], describes the required input of data and parameters. Ward et al. [1984a], and [1984b] describe the comparison of the results from the SWIFT code with field data and other existing codes. This document is devoted to assisting the analyst who desires to use the SWIFT II code. The analyst is referred to the User's Manual for SWIFT II (Reeves et al. [1986b]) for detailed data input instructions. Eight examples are presented to illustrate the use of SWIFT II. The implementation of the numerical simulation of the physical problem is described for each example. For each problem, a listing of the input data and a microfiche listing of the output are provided.

14 DOCUMENT ANALYSIS - a. KEYWORDS/DESCRIPTORS

radionuclide transport
computer code
self-teaching curriculum
ground-water flow

b. IDENTIFIERS/OPEN-ENDED TERMS

15 AVAILABILITY STATEMENT

Unlimited

16 SECURITY CLASSIFICATION

(This page) Unclassified

(This report) Unclassified

17 NUMBER OF PAGES

18 PRICE

☆ U.S. GOVERNMENT PRINTING OFFICE: 1987-172-511

ABSTRACT

Several documents have been written describing SWIFT II, the most current version of the SWIFT (Sandia Waste Isolation Flow and Transport) code. Reeves et al. [1986a], describes the theory and implementation, and Reeves et al. [1986b], describes the required input of data and parameters. Ward et al. [1984a] and [1984b] describe the comparison of the results from the SWIFT code with field data and other existing codes. This document is devoted to assisting the analyst who desires to use the SWIFT II code. The analyst is referred to the user's Manual for SWIFT II (Reeves et al. [1986b]) for detailed data input instructions. Eight examples are presented to illustrate the use of SWIFT II. The implementation of the numerical simulation of the physical problem is described for each example. For each problem, a listing of the input data and a microfiche listing of the output are provided.

TABLE OF CONTENTS

LIST OF FIGURES

LIST OF FIGURES (Continued)

LIST OF TABLES

1. INTRODUCTION

The SWIFT (Sandia Waste-Isolation Flow and Transport) computer code was developed for use in simulating the transport of radionuclides dissolved in groundwater. It is a finite-difference, transient, three-dimensional code which, in addition to radionuclide transport, solves the coupled equations for fluid flow, heat transfer, and brine transport in saturated porous media. It evolved from the U.S. Geological Survey code SWIP (Survey Waste Injection Program) (INTERCOMP, 1976) and has undergone several modifications since its development (Dillon et al., 1978, Reeves and Cranwell, 1981, and Reeves et al., 1986a and b). The current version, referred to as SWIFT II, has the capability of treating three additional systems; two are confined dual-porosity systems, one of which is a fractured porous material, and the other an aquifer with conductive confining beds. The third system is an unconfined aquifer with a free water surface.

The purpose of this document is to familiarize the reader with the SWIFT II code through a set of sample problems. Eight problems are presented demonstrating the added capabilities of SWIFT II. The first three problems demonstrate the solute transport through dual porosity media capability of SWIFT II. The following problem (Problem 4) demonstrates the capability of SWIFT II to analyze the fluid flow in a dual-porosity media. The next two problems (Problems 5 and 6) demonstrate the capability of SWIFT II to simulate fluid flow and heat transfer through an aquifer with confining beds. The last two problems (Problems 7 and 8) demonstrate the capability of SWIFT II to treat problems involving free water surfaces. In each case, the discussion begins with a physical description of the problem followed by a description of the numerical simulation. For convenience, the nomenclature for all the problems is presented in Section 6. This document is meant to be used together with two other documents describing the theory [Reeves et al., 1986a] and data-input requirements [Reeves et al., 1986b] of the SWIFT II code. These documents are referenced simply as the Theory and Implementation and the Data-Input Guide, respectively, throughout this report.

2. SOLUTE TRANSPORT THROUGH DUAL POROSITY MEDIA

2.1 PROBLEM 1. TRANSPORT OF A DECAYING RADIONUCLIDE IN FRACTURED POROUS MEDIA [TANG ET AL, 1981].

2.1.1 Objective

The objective of Problem 1 is to illustrate radionuclide transport through fractured media using a prismatic characterization of the rock matrix.

2.1.2 Description of the Problem

Problem Statement. A thin, rigid fracture is situated within a saturated porous rock matrix as shown in Figure 2.1-1. Both the fracture and matrix are semi-infinite in their extent. Radionuclides, which derive from a source of constant strength, are convected and dispersed through the fracture in a constant velocity field and are diffused into the rock matrix.

Transport Equations. The transport within the fractures is given by the equation:

$$\frac{\partial}{\partial x}(\rho C u) + \frac{\partial}{\partial x}\left(\rho D \frac{\partial C}{\partial x}\right) - \Gamma - \lambda K \phi \rho C = \frac{\partial}{\partial t}(K \phi \rho C) \quad . \qquad (2.1\text{-}1)$$

Transport within the rock matrix is assumed to occur perpendicular to the fracture and is governed by the equation:

$$\frac{\partial}{\partial s}\left(\rho' D'_m \frac{\partial C'}{\partial s}\right) + \Gamma - \lambda K' \phi' \rho' C' = \frac{\partial}{\partial t}(K' \phi' \rho' C') \quad , \qquad (2.1\text{-}2)$$

where s is the one-dimensional coordinate for the local (matrix) units.

At the fracture/matrix interface the flux is continuous, thus

$$\Gamma = - A_V \rho' D'_m \left.\frac{\partial C'}{\partial s}\right|_{s=0} \quad . \qquad (2.1\text{-}3)$$

The mixed parameters are defined in terms of fundamental parameters. The dispersion/diffusion in the fracture is:

$$D = \alpha_L u + D_m \qquad (2.1\text{-}4a)$$

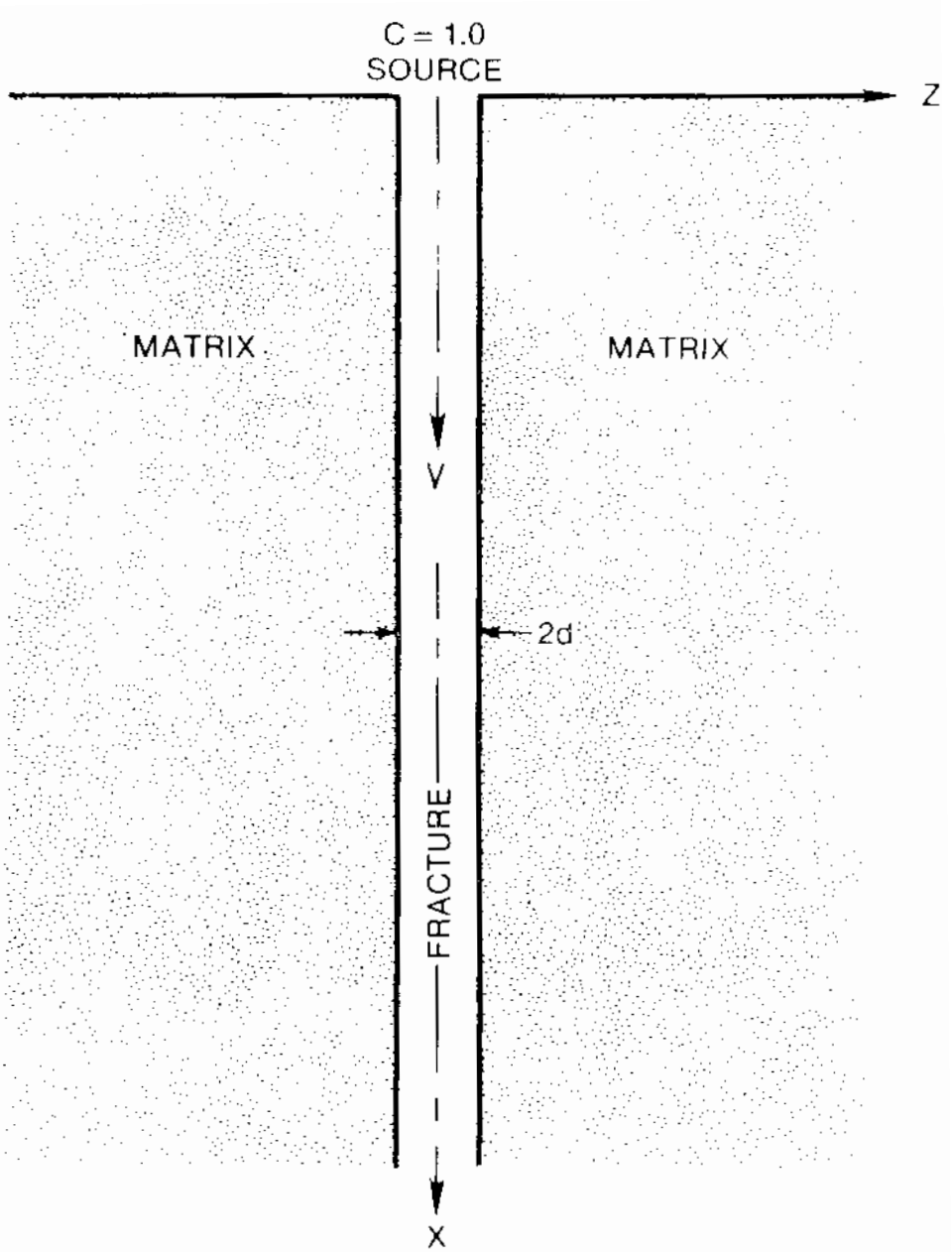

Figure 2.1-1. Problem 1. Schematic Diagram

with the diffusivity in the fractures being

$$D_m = \phi D^* \qquad (2.1\text{-}4b)$$

and the diffusivity in the rock matrix being

$$D'_m = \tau\phi' D^* \quad . \qquad (2.1\text{-}4c)$$

Other parameters are defined in Section 6.

Initial/Boundary Conditions. Within the rock matrix the initial/boundary conditions are

$$C'(x,s,0) = 0 \qquad (2.1\text{-}5a)$$

and

$$C'(x,\infty,t) = 0 \qquad (2.1\text{-}5b)$$

At the fracture/matrix interface the fracture and matrix concentrations are equal:

$$C'(x,0,t) = C(x,t) \qquad (2.1\text{-}5c)$$

Within the fracture the initial/boundary conditions are

$$C(x,0) = 0 \qquad (2.1\text{-}6a)$$

and

$$C(0,t) = 1 \qquad (2.1\text{-}6b)$$

The numerical treatment of the unit concentration at the inlet (equation 2.1 - 6b) in the input is discussed in detail in Problem 2.

Input/Output Specifications. The data for this problem, given in Table 2.1-1, is the same as that prescribed by Tang et al. [1981, p. 561 ff] for their low velocity case. Curves of concentration versus distance within the fracture

are obtained for times of 100, 1000, and 10,000 days. A single curve of concentration versus distance within the rock matrix is desired for t = 10,000 days and x = 1.5 m.

2.1.3 Numerical Simulation

Discussion of Code Input. The region used for the numerical solution must be larger than the zone of contaminant migration in order to use a finite domain to represent a semi-infinite one. To estimate the extent of migration, the steady state solution of Tang et al., (1981) was used. They provide a solution for a characteristic length ($\tilde{L}$) of penetration into the fracture and another for penetration into the rock matrix ($\tilde{a}$). For a relative concentration of 0.368 in both the fracture and the matrix:

$$\tilde{L} = - \{1/(2\alpha_L) - [1/(4\alpha_L^2) + \psi/D]^{1/2}\}^{-1} \qquad (2.1\text{-}7)$$

and

$$\tilde{a} = (D'/\lambda)^{1/2} \qquad (2.1\text{-}8)$$

where

$$D = \alpha_L v + D^* \qquad (2.1\text{-}9a)$$

$$D' = \bar{\tau} D^* \qquad (2.1\text{-}9b)$$

$$\psi = \lambda + \phi'(D'\lambda)^{1/2}/d \quad . \qquad (2.1\text{-}9c)$$

From values in Table 2.1-1, these expressions give

$$\tilde{L} = 1.4 \text{ m} \qquad (2.1\text{-}10)$$

and

$$\tilde{a} = 0.30 \text{ m} \quad . \qquad (2.1\text{-}11)$$

Table 2.1-1

Problem 1. Data

Parameter	Symbol	Value
Fracture Width	$2d$	10^{-4} m
Matrix Porosity	ϕ'	0.01
Matrix Tortuosity	τ	0.1
Fracture Dispersivity	α_L	0.5 m
Molecular Diffusion in Water	D^*	1.6×10^{-5} cm ^{2}/s
Half Life	τ	12.35 y
Decay Constant	λ	0.0561 y^{-1}
Matrix Retardation	K'	1.0
Fracture Retardation	K	1.0
Fracture Velocity	v	0.01 m/d
Fracture Porosity	ϕ	1.0

The domains of the simulation are larger than those given in Equations (2.1 10 and 2.1 11):

$$L = 10.24 \text{ m} \qquad (2.1\text{-}12)$$

and

$$a = 1.2 \text{ m} \quad . \qquad (2.1\ 13)$$

Spatial increments in the fracture and matrix domains are taken to be significantly smaller than the characteristic lengths. Some numerical experimentation is necessary for determining the optimum spatial and temporal increment size. There is, however, one numerical criterion:

$$\Delta S \sim (2D'\Delta t)^{1/2} \qquad (2.1\ 14)$$

for the matrix, which is a useful guide [see Reeves et al. 1986a]. The adopted gridding is shown in Figures 2.1 2 and 2.1-3 and the input data are listed in Figure 2.1-4. An interconnected mesh is used to simulate the composite fracture/matrix system with the individual increments specified in Cards R1-17 (Δx), R1-18 (Δy), and R1-19 (Δz) (see Figure 2.1-4). This mesh is called the global grid. The rock matrix is simulated by attaching a one-dimensional grid to each of the global blocks. Each of these grids is referred to as a local block. Note that global grid block 1 does not have a local block attached to it, as the former is used to establish the constant inlet concentration. Therefore, local block 1 is attached to global block 2, local block 2 to global block 3, etc. This gridding is specified by the three parameter values provided in Cards ROD-2 (n) and RID-2-2 (a and Δs). Given the number of increments n_s and the increment Δs at the fracture/matrix interface, these grids were generated automatically. Note that the local blocks are connected only to the global blocks and not to each other.

Another problem specification that requires explanation is the manner in which the fracture velocity is described. The flow is not directly specified in the SWIFT II code. In order to arrive at the fracture velocity, the flow within the global system is maintained using injection and production wells at each end of the grid. The imposed flow is:

$$q = 2d\Delta yv = 1.157 \times 10^{-11} \text{ m}^3/\text{s}, \quad \text{R2-6} \quad . \qquad (2.1\text{-}15)$$

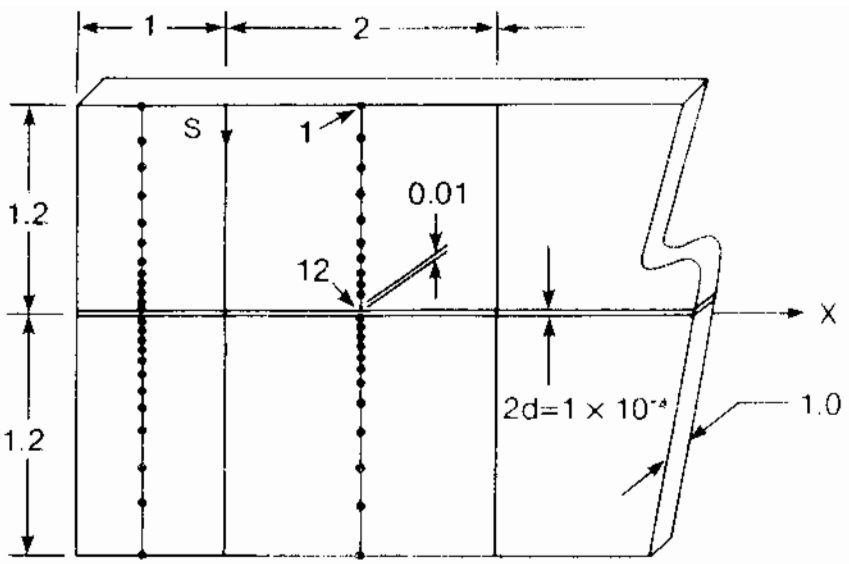

Figure 2.1-2. Problem 1. Prismatic Gridding Where Block Numbering Corresponds to Local Blocks

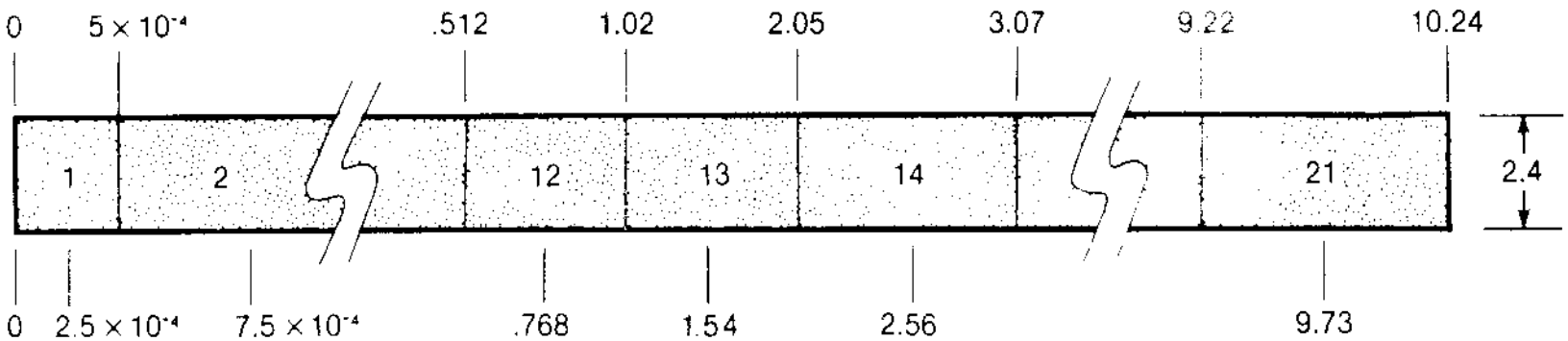

Figure 2.1-3. Location of Global Grid Block Boundaries and Centers

```
PROBLEM NO. 1, THREE-COMPONENT NUCLIDE TRANSPORT IN FRACTURED MEDIA,  M-1-1
03/86, COMPARISON WITH ANALYTICAL SOL'N - PRISMATIC REPRESENTATION     M-1-2
    4     0     0     0     0     0     0     1     0                  M-2
   21     1     1     2     1     2     0     2     1     0     1     0     0     0M 3-1
    0     2     1     0                                                M-3-2
ECORAD CPAC         1     0     0      12.35                           RO-1
       0 0                                                           RO-2-1
       0 0                                                           RO-2-1
       1 0                                                           RO-2-2
       1 0                                                           RO 2-2
    0                                                                ROD-1
   12                                                                ROD-2
    3    21     1     1     1     1     1     6                       ROD-3
                                                                      ROD-3-BLN
       0.0         0.0         0.0     4186 0         1.0                  R1-1
       0.0         0.0         0.0        0 0        0 50        0 06 6672E-14R1-2
       0.0         0 0         0.0                                         R1-2.5
       0.5         0.0                                                     R1-2.5
       0.0         0.0         0.0                                         R1-2.5
  4 00E08          0.0                                                     R1-2.5
    2700.0   1 013E05          20.0      1000.0      1000.0                 R1-3
    2    2     2    2                                                     R1-6
      20.0       0.001         20.0       0.001                          R1-7
      0.20       0 001         0.80       0.001                          R1-8
     100.0       0.001        200.0       0.001                          R1-9
     100.0       0.001        200.0       0.001                          R1-10
       0 0        20.0                                                   R1-11
     100.0        20.0                                                   R1 11
    0     0                                                             R1-17
      20.0   1.013E05           0.0         0.0                          R1 16
 2*5.0E-4      1.0E-3      2.0E-3      4.0E-3      8.0E-3     1.6E 2     3.2E-2
   6.4E-2       0.128       0.256       0.512     9*1.024
      1.0
      2.4
3.4052E-7   3.4052E-7   3.4052E-7   4.167E-5         0.0         0.0          0.0R1-20
                                                                            R1-21
   1     1     1     1     1     1                                          R1-26-1
       1.0         1.0         1.0         1.0         0.0         0.01.91985E09R1-26-2
       0.0         0.0         0.0                                         R1-26-3
                                                                           R1-26 BLN
    0     0                                                               R1-27
1.00E-50                                                                  R1D 1
1.60E-12         0.0       0.010     1.5E-15         0 0         1.0          1.0R1D-2-1
   1     1         1.2       0.010         0.0                           R1D 2-2
                                                                          R1D-3-BLN
       0.0                                                                R1D-4
                                                                          R1D-5-BLN
    0     0     1                                                        I-1
    1     1     1     1     1     1         1.0                          I-4
                                                                         I-4 BLN
```

Figure 2.1 4. Problem 1. Listing of GWIFT 11 Input Data

```
  2   21    1    1    1    1    1                                        R1A-1
  1    1    1    1    1    1    2                                        R1A-1
                                                                        R1A-1-BLN
    0 0                                                                 R1A-2
  2    1    1    0    0    0    0    0    0                            R2-1
+1       0.50                                                          R2-2
  2                                                                     R2-4
 1.1 15/E-11                                                            R2-6-1
 2+1.157E-11                                                            R2-6-2
                                                                        R2-6-BLN
  1    1    1    1    1    1                                          R2-7-1
    1 0       0.0      20 0       0 0                                 R2-7-2
  2   21    1    1    1    1                                          R2-7-3
    1.0       0.0      20.0       0 0                                 R2-7-4
                                                                        R2-7-BLN
    1.0       1.0
  1    1    1    1    1    1  000    0 0000    0   13    1  000   12R2-13
  0    0    0    0    1    0    0    0    1                           R2-1
  1                                                                     R2-9
  1    1    1    1                                                    R2-10-1
    0.0       0.0-7.1212E-5                                           R2-10-2
                                                                        R2-10-BLN
  3                                                                     R2-11.5
3.456E06  3.456E06
  1   -1   -1   -1   -1   -1  000    0 0000    0   10   -1  000   10R2-13
  0    0    0    0    0    0    0    0    0                           R2-1
 8.64E06  5.184E06
  1   -1   -1   -1    1   -1  000    0 0000    0   10    1  000   10R2-13
  0    0    0    0    0    0    0    0    0    0                      R2-1
1.525E07  6.910E06
  1   -1   -1   -1   -1   -1  000    0 0000    0   10   -1  000   10R2-13
  0    0    0    0    0    0    0    0    0    0                      R2-1
2.502E07  9.771E06
  1   -1   -1   -1   -1   -1  000    0 0000    0   10   -1  000   10R2-13
  0    0    0    0    0    0    0    0    0    0    0                 R2-1
3.884E07  1.382E07
  1   -1   -1   -1   -1   -1  000    0 0000    0   10   -1  000   10R2-13
  0    0    0    0    0    0    0    0    0    0                      R2-1
5.838E07  1.954E07
  1   -1   -1   -1   -1   -1  000    0 0000    0   10   -1  000   10R2-13
  0    0    0    0    0    0    0    0    0    0                      R2-1
8.640E07  2.802E07
  1   -1   -1   -1    1   -1  000    0 0000    0   10    1  000   10R2-13
  0    0    0    0    0    0    0    0    0    0                      R2-1
1.251E08  3.906E07
  1   -1   -1   -1   -1   -1  000    0 0000    0   10   -1  000   10R2-13
  0    0    0    0    0    0    0    0    0    0                      R2-1
1.803E08  5.522E07
  1   -1   -1   -1   -1   -1  000    0 0000    0   10   -1  000   10R2-13
  0    0    0    0    0    0    0    0    0    0                      R2-1
```

Figure 2.1-4. Problem 1. Listing of SWIFT II Input Data (Continued)

```
2.584E08  7.810E07
  1    -1    -1    -1    -1    -1   000     0 0000    0    10    -1   000    10R2-13
  0     0     0     0     0     0     0     0    0    0                        R2-1
3.448E08   8.64E07
  1    -1     1    -1    -1    -1   000     0 0000    0    10    -1   000    10R2-13
  0     0     0     0     0     0     0     0    0    0                        R2-1
4.312E08   8.64E07
  1    -1    -1    -1    -1     1   000     0 0000    0    10    -1   000    10R2-13
  0     0     0     0     0     0     0     0    0    0                        R2-1
5.176E08   8.64E07
  1    -1    -1    -1     1    -1   000     0 0000    0    10    -1   000    10R2-13
  0     0     0     0     0     0     0     0    0    0                        R2-1
6.040E08   8.64E07
  1    -1    -1    -1    -1    -1   000     0 0000    0    10    -1   000    10R2-13
  0     0     0     0     0     0     0     0    0    0                        R2-1
6.904E08   8.64E07
  1    -1    -1    -1    -1    -1   000     0 0000    0    10     1   000    10R2-13
  0     0     0     0     0     0     0     0    0    0                        R2-1
7.767E08   8.64E07
  1    -1    -1    -1    -1    -1   000     0 0000    0    10    -1   000    10R2-13
  0     0     0     0     0     0     0     0    0    0                        R2-1
8.640E08  8 730E07
  1    -1    -1    -1     1    -1   000     0 0000    0    10     1   000    10R2-13
  0     0     0     0     0     0     0     0    0    0                        R2-1
1.728E09  1 728E08
  1    -1    -1    -1     1    -1   000     0 0000    0    10     1   000    10R2-13
  0     0     0     1                                                        R2-1-STOP
```

Figure 2.1 4. Problem 1. Listing of SWIFT II Input Data
(Continued)

Since both fracture and matrix are included within the global blocks (IFD = 0 in Card ROD 3), the global porosity is specified as

$$\phi = d/(a+d) = 4.167 \times 10^{-5}, \quad \text{R1-20} \quad . \qquad (2.1\text{-}16)$$

This global porosity yields, from Equation (2.1-4b), the value

$$D_m = 6.6672 \times 10^{-14} \ m^2/s, \quad \text{R1-2} \quad , \qquad (2.1\text{-}17a)$$

for the diffusion of the global system. The corresponding relation for the rock matrix is, from Equation (2.1-4c):

$$D'_m = 1.6 \times 10^{-12} \ m^2/s \quad . \qquad (2.1\text{-}17b)$$

Results. The numerical results obtained from the SWIFT II code are compared to the analytical solutions of Tang et al. (1981) in Figures 2.1-5 and 2.1-6. Both within the fracture and the matrix, the two agree reasonably well.

Discussion of the Code Output. The code output is presented in the microfiche listing (inside the back cover). The tables which are denoted in the microfiche by the words "dual porosity" or "rock matrix" refer to the rock matrix portion of a fracture/matrix system. In Problems 6 and 7, however, these tables refer to the confining beds of an aquifer.

In the table entitled "X-Direction Distance to Grid-Block Center" the distances along the fracture to the centers of the grid blocks are given. The distance x = 1.5 m lies in Global Block 13. The second table, "Local Unit Numbers," provides identifiers for the local blocks imbedded in the global blocks. No local blocks are imbedded in Block 1. This block is used only to establish a constant-concentration boundary within the fracture. Local Block 12 is associated with Global Block 13 which is 1.5 m down the fracture. A third table, "Local Subsystem Discretization Parameters," gives nodal locations within the rock matrix or local blocks. Node 12 is located at the fracture/matrix interface. Thus, for example, Node 4 is located at a distance of about 0.4 m from that interface.

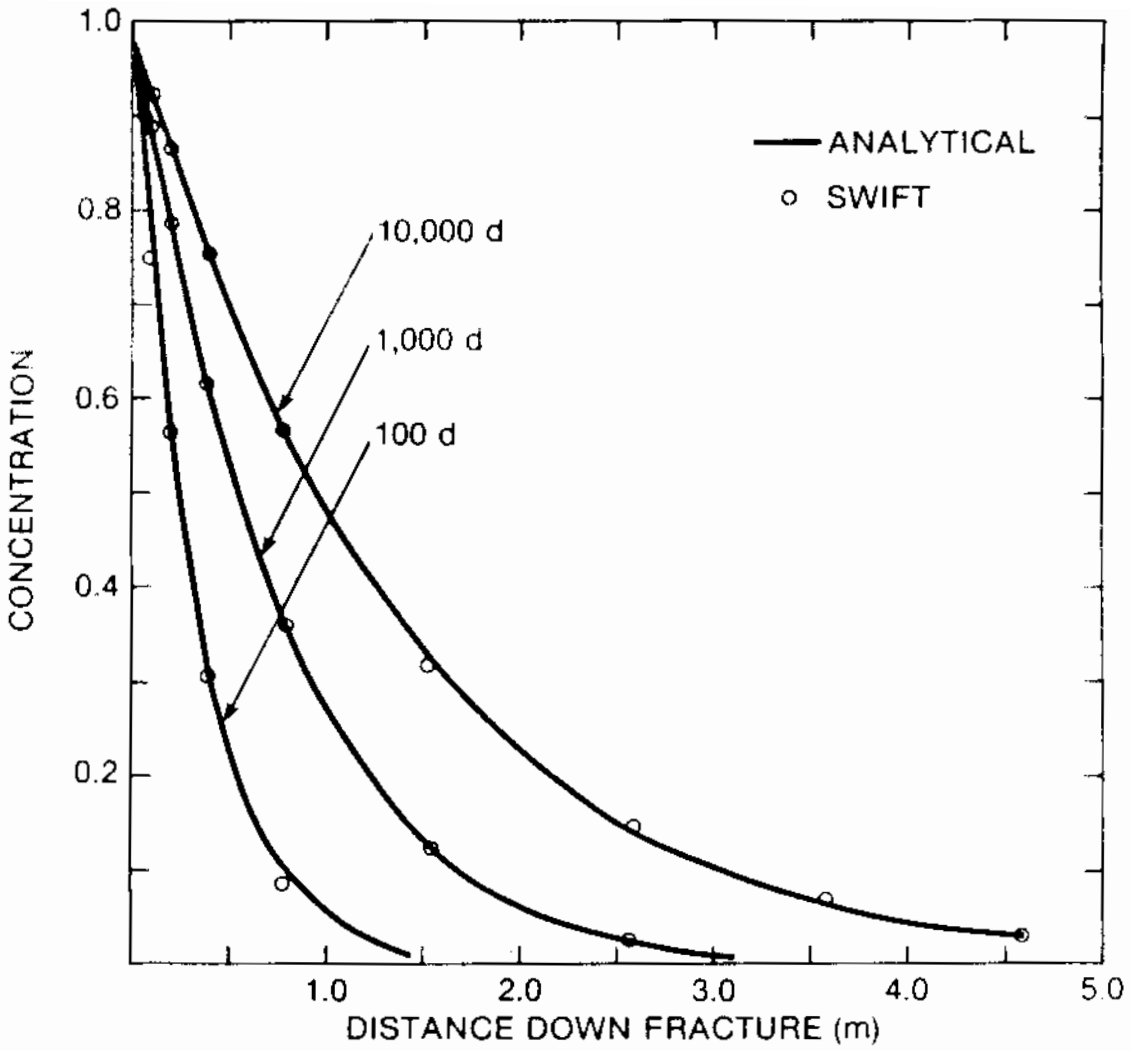

Figure 2.1-5. Radionuclide Concentrations Within the Fracture for a Prismatic Characterization of the Rock Matrix

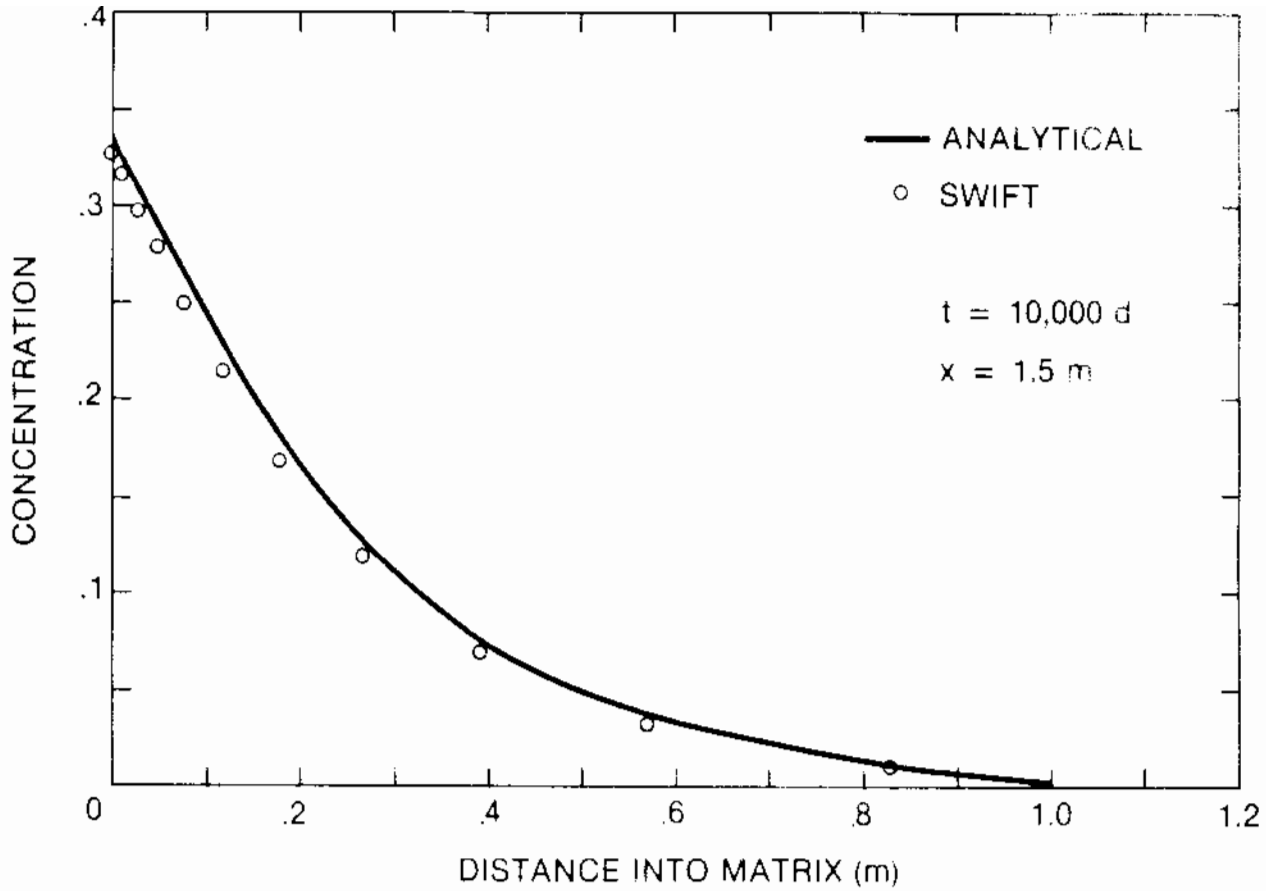

Figure 2.1-6. Radionuclide Concentrations Within the Rock Matrix for a Prismatic Characterization of the Rock Matrix

Tables of fracture concentrations, labelled "Component-1 Concentration," and matrix concentrations, labelled "Component-1 Radionuclide Concentration Within the Rock Matrix," are presented on the microfiche listing for up to 10,000 days at selected time intervals.

2.2 PROBLEM 2. TRANSPORT OF A DECAYING RADIONUCLIDE IN FRACTURED POROUS MEDIA [HUYAKORN, 1983; RASMUSON, 1984]

2.2.1 Objective

The objective of Problem 2 is to illustrate radionuclide transport of a decaying radionuclide through fractured media using a spherical characterization of the rock matrix.

2.2.2 Description of the Problem

This problem is identical to Problem 1 with only two exceptions. First, the exposed surface area per unit fracture length between fracture and matrix is assumed to be larger and is therefore approximated by a spherical surface (Figure 2.2-1) for the rock matrix. Thus, Equation (2.1-2) in the previous section is replaced by

$$\frac{1}{s}\frac{\partial}{\partial s}\left(s\rho' D'_m \frac{\partial C'}{\partial s}\right) + \Gamma - \lambda K'\phi'\rho' C' = \frac{\partial}{\partial t}(K'\phi'\rho' C') \quad . \qquad (2.2\text{-}1)$$

The radius for the spherical units is chosen to be identical to that used in Problem 1 for the length of the prismatic units:

$$a = 1.2 \text{ m} \quad . \qquad (2.2\text{-}2)$$

Second, the matrix diffusion is reduced:

$$D'_m = 5.787 \times 10^{-13} \text{ m}^2/\text{s} \qquad (2.2\text{-}3)$$

to be consistent with Huyakorn's (1983) work. Also, the calculated concentrations are output at t = 441, 3619, and 90,615 d, both within the fracture and the rock matrix. The position for the distribution within the rock matrix is changed to x = 1.0 m.

2.2.3 Numerical Simulation

Discussion of the Code Input. To simulate the semi-infinite fracture, two boundary conditions are specified. The edge of the system (10.24 m), a convection-only condition

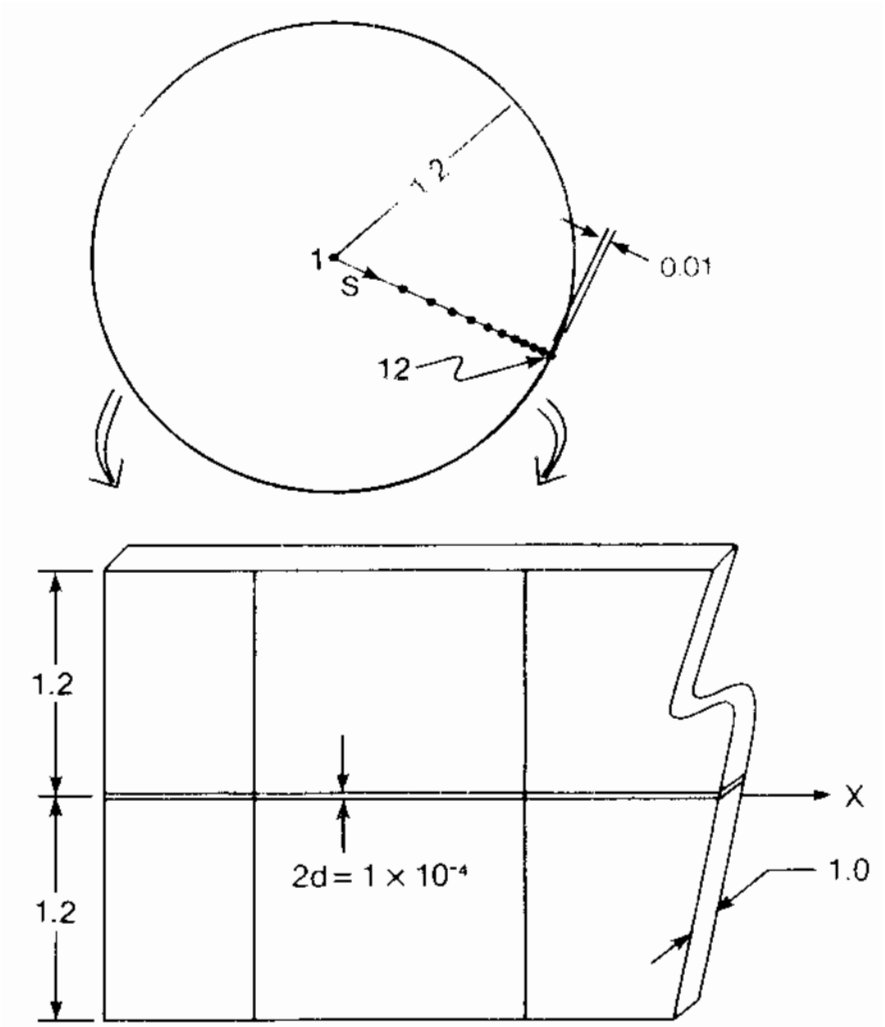

Figure 2.2-1. Problem 2. Spherical Gridding

$$\left.\frac{\partial C}{\partial x}\right|_{x=L} = 0 \qquad (2.2\text{-}4)$$

is the default condition (Figure 2.1-1).

A unit concentration at the inlet (Equation 2.1-6b) cannot be specified directly. Because SWIFT II was designed to evaluate repository-site performance, only facilities for radionuclide sources have been provided. However, a constant-concentration boundary condition may be implemented by defining the inlet block as an essentially infinite well-mixed reservoir. Distances are then measured by taking $x = 0$ at the interface between Blocks 1 and 2, and the dual-porosity region begins with Block 2 (see Card ROD-3). To simulate a well-mixed reservoir, four steps are taken.

First, the thickness of Block 1 is increased to

$$\Delta z_1 = (1.91985 \times 10^{9} + 2.4)\text{m}, \quad \text{R1-26-2} \qquad (2.2\text{-}5a)$$

using the modification cards. Second, the concentration of this block is specified as

$$C_1 = 1, \quad \text{I-4} \quad . \qquad (2.2\text{-}5b)$$

Third, a source is used to replace the mass lost from the reservoir by both decay and convection:

$$Q = C_1\rho(\lambda\phi\Delta x_1\Delta y_1\Delta z_1 + q) = 7.12 \times 10^{-5} \text{ kg/s}, \quad \text{R2-10} \quad . \qquad (2.2\text{-}5c)$$

The other component terms are prescribed in Cards R1-6 (ρ), RO-1 ($\tau = \ell n(2)/\lambda$), R1-20 (ϕ), R1-17 (Δx_1), R1-18 (Δy_1) and R2-6 (q).

Fourth, to implement the "well-mixed" reservoir, the dispersivity

$$\alpha_{L1} = 4 \times 10^{8} \text{ m}, \quad \text{R1-2.5-2} \qquad (2.2\text{-}5d)$$

is defined for Block 1. This value is large enough to allow unrestricted communication between Blocks 1 and 2. This dispersivity is assigned to Rock-Type 2 which is ascribed in R1A-1 to Block 1. Rock-Type 1, with α_L = 0.5 m, refers to the transporting region of the fracture, blocks 2 through 21. A complete listing of the input data is given in Figure 2.2-2.

Results. The results obtained from the SWIFT II code are compared to those of Huyakorn's (1983) finite-element code FTRANS and the analytic solution of Rasmuson (1984) in Figures 2.2-3 and 2.2-4. Transport within the fracture is retarded more when the spherical matrix characterization is used. In spite of a reduction by approximately 3 in the matrix diffusivity, the spherical characterization yields a retardation that is greater by a factor of 3 or more than that for the prismatic characterization.

Code Output. The results are partly dependent on the convective velocity and the constant-concentration inlet boundary condition. To check these, the reader is referred to the microfiche listing. The convective velocity is equal to the Darcy velocity divided by the porosity. The value of porosity for the global system ($\phi = 4.167 \times 10^{-5}$) is given in the table entitled "Specification of Homogeneous Global System." A constant Darcy velocity is obtained by including an injection well at the inlet and a discharge well at the outlet. These wells are listed at GRID H 05 of the microfiche. The fluxes listed there are divided by the cross-sectional area of the global system to obtain the Darcy velocity listed in the table entitled "Global X-Dir - Darcy Velocity - (m/sec)." The convective velocity is calculated as:

$$v = u/\phi = (4.8208 \times 10^{-12}/4.167 \times 10^{-5})\ m/s = 0.01\ m/d \qquad (2.2\text{-}6)$$

which is consistent with the problem specifications (Table 2.1-1).

The constant-concentration inlet boundary condition is verified by examining the radionuclide concentration tables labelled "Component-1 Concentration." There are several such tables, which are displayed at selected time intervals up to t = 90,615 d. In each case, the C = 1.000 condition is maintained to at least four significant figures.

```
PROBLEM NO. 2, THREE-COMPONENT NUCLIDE TRANSPORT IN FRACTURED MEDIA,  M-1-1
03/86, COMPARISON WITH 'FTRANS' -- SPHERICAL REPRESENTATION           M-1-2
     4     0     0     0     0     0     0     1     0                 M-2
    21     1     1     2     1     2     0     2     1     0     1     0     0     0M-3-1
     0     2     1     0                                               M-3-2
100RAD  00.                1     0     0    12.350                     RO-1
        3.0                                                           RO-2-1
        0.0                                                           RO-2-1
        1.0                                                           RO-2-2
        1.0                                                           RO-2-2
     0     0                                                          ROD-1
    12                                                                ROD-2
     2     1     1     1     1     1     1     0                       ROD-3
                                                                      ROD-3-BLN
        0.0         0.0         0.0      4186.0         1.0          R1-1
        0.0         0.0         0.0         0.0        0.50      0.0  1.00E-30R1-2
        0.0         0.0         0.0                                  R1-2.5-1
       0.50         0.0                                              R1-2.5-2
        0.0         0.0         0.0                                  R1-2.5-1
   4.00E08          0.0                                              R1-2.5-2
     2700.0    1.013E05        20.0      1000.0      1000.0          R1-3
     2     2     2     2                                             R1-6
       20.0       0.001        20.0       0.001                     R1-7
       0.20       0.001        0.80       0.001                     R1-8
      100.0       0.001       200.0       0.001                     R1-9
      100.0       0.001       200.0       0.001                     R1-10
        0.0        20.0                                             R1-11
      100.0        20.0                                             R1-11
     0     0                                                         R1-12
       20.0    1.013E05         0.0         0.0                     R1-16
  2*5.0E-4       1.0E-3      2.0E-3      4.0E-3      8.0E-3     1.6E-2     3.2E-2
     6.4E-2       0.128       0.256       0.512    9*1.024
        1.0
        2.4
3.4052E-07  3.4052E-7  3.4052E-7   4.167E-5         0.0         0.0          0.0R1-20
                                                                      R1-21
     1     1     1     1     1     1                                  R1-26-1
        1.0         1.0         1.0         1.0         0.0         0.01.91985E09R1-26-2
        0.0         0.0         0.0                                  R1-26-3
                                                                     R1-26-BLN
     0     0                                                         R1-27
  1.00E-20                                                           R1D-1
5.7870E-13          0.0       0.010         0.0         0.0         1.0       1.0R1D-2-1
     0     1         1.2      0.0100                                 R1D-2-2
                                                                     R1D-3-BLN
        0.0                                                          R1D-4
                                                                     R1D-5-BLN
     0     0     1                                                   I-1
     1     1     1     1     1     1         1.0                     I-4
                                                                     I-4-BLN
     2    21     1     1     1     1     1                           R1A-1
     1     1     1     1     1     1     2                           R1A-1
                                                                     R1A-1-BLN
        0.0         0.0                                              R1A-2
```

Figure 2.2-2. Problem 2. Listing of SWIFT II Input Data

```
  2     1     1     0     0     0     0     0     0                                  R2-1
 +1        0.50                                                                    R2-4
  2                                                                                R2-4
  1-1.157E-11                                                                      R2-6-1
  2+1.157E-11                                                                      R2-6-2
                                                                                   R2-6-BLN
  1     1     2     1     1     1                                                  R2-7-1
     1.0         0.0         20.0         0.0                                     R2-7-2
  2    21     1     1     1     1                                                  R2-7-1
     1.0         0.0         20.0         0.0                                     R2-7-2
                                                                                   R2-7-BLN
     0.0         0.0
  0     0     0     0     0     0   000     0 0000     0    13    11   000    12R2-13
  0     0     0     0     1     0     0     0     1                                R2-1
  1
  1     1     1     1                                                            R2-10-1
     0.0         0.0-7.1212E-5                                                   R2-10-2
                                                                                   R2-10BLN
  3                                                                                R2-11-1
 8.64E06    8.64E06
  1    -1    -1    -1    -1    -1   000     0 0000     0    00    -1   111    00R2-13
  0     0     0     0     0     0     0     0     0                                R2-1
2.086E07   1.222E07
 -1    -1    -1    -1    -1    -1   000     0 0000     0    00     1   111    00R2-13
  0     0     0     0     0     0     0     0     0                                R2-1
3.813E07   1.727E07
  1    -1    -1    -1     1    -1   000     0 0000     0    00     1   111    00R2-13
  0     0     0     0     0     0     0     0     0                                R2-1
6.256E07   2.443E07
 -1    -1    -1    -1    -1    -1   000     0 0000     0    00     1   111    00R2-13
  0     0     0     0     0     0     0     0     0                                R2-1
9.710E07   3.454E07
  1    -1    -1    -1     1    -1   000     0 0000     0    00     1   111    00R2-13
  0     0     0     0     0     0     0     0     0                                R2-1
1.459E08   4.884E07
 -1    -1    -1    -1    -1    -1   000     0 0000     0    00    -1   111    00R2-13
  0     0     0     0     0     0     0     0     0                                R2-1
2.150E08   6.906E07
 -1    -1    -1    -1    -1    -1   000     0 0000     0    00    -1   111    00R2-13
  0     0     0     0     0     0     0     0     0                                R2-1
3.126E08   9.765E07
  1    -1    -1    -1     1    -1   000     0 0000     0    00     1   111    00R2-13
  0     0     0     0     0     0     0     0     0                                R2-1
4.507E08   1.381E08
 -1    -1    -1    -1    -1    -1   000     0 0000     0    00    -1   111    00R2-13
  0     0     0     0     0     0     0     0     0                                R2-1
6.439E08   1.952E08
 -1    -1    -1    -1    -1    -1   000     0 0000     0    00    -1   111    00R2-13
  0     0     0     0     0     0     0     0     0                                R2-1
9.220E08   2.761E08
  1    -1    -1    -1     1    -1   000     0 0000     0    00    -1   111    00R2-13
  0     0     0     0     0     0     0     0     0                                R2-1
1.313E09   3.904E08
  1    -1    -1    -1    -1    -1   000     0 0000     0    00    -1   111    00R2-13
```

Figure 2.2-2. Problem 2. Listing of SWIFT II Input Data (Continued)

```
  0     0     0     0     0     0     0     0     0                                  R2-1
1.864E09  5.520E08
 -1    -1    -1    -1    -1    -1   000     0 0000     0    00    -1   111    00R2-13
  0     0     0     0     0     0     0     0     0                                  R2-1
2.645E09  7.805E08
 -1    -1    -1    -1    -1     1   000     0 0000     0    00    -1   111    00R2-13
  0     0     0     0     0     0     0     0     0                                  R2-1
7.829E09  8.640E08
  1    -1    -1    -1     1    -1   000     0 0000     0    00     1   111    00R2-13
  0     0     0     1     0     0     0     0     0                                  R2-1-STOP
```

Figure 2.2-2. Problem 2. Listing of SWIFT II Input Data (Continued)

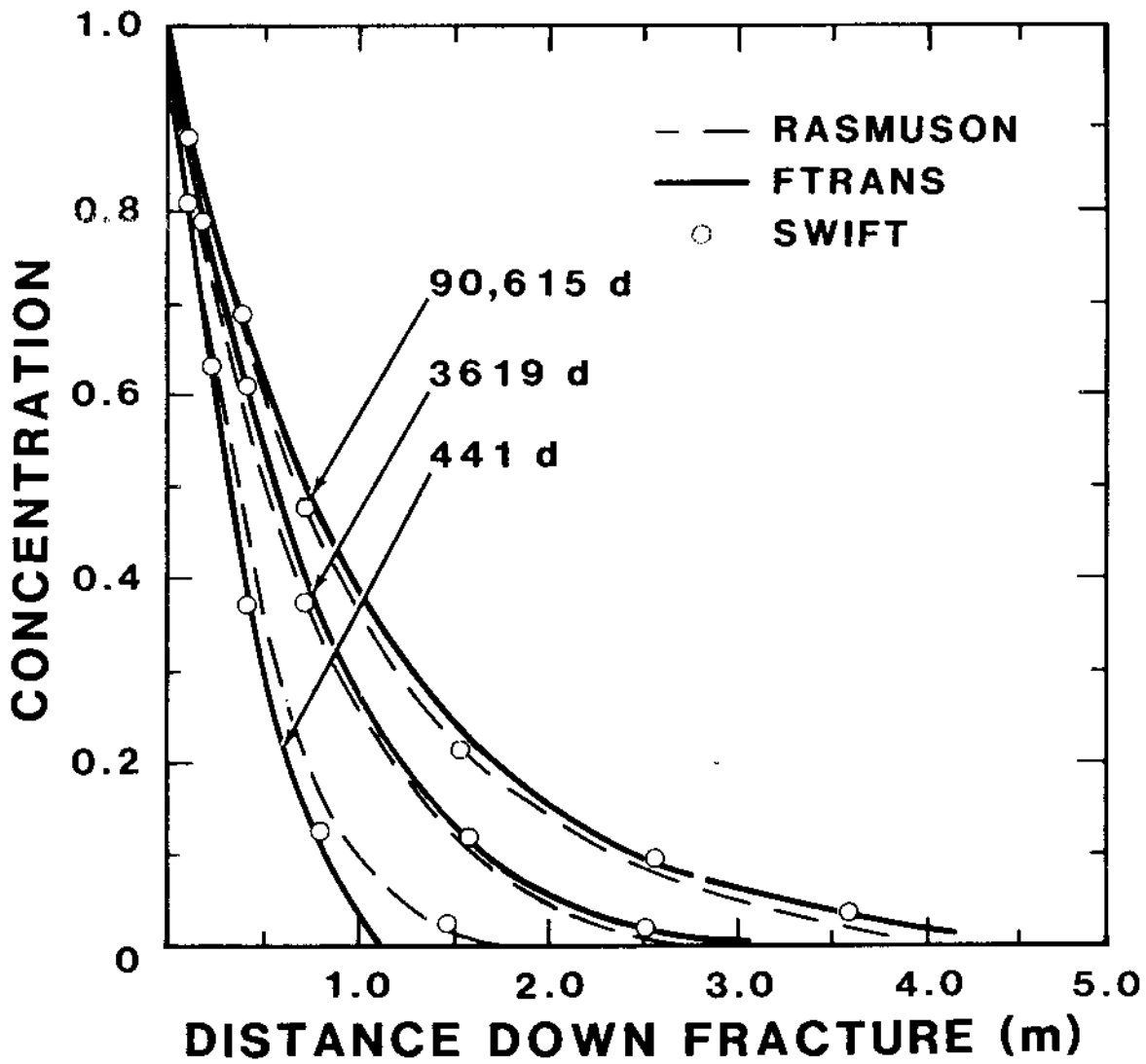

Figure 2.2-3. Radionuclide Concentrations Within the Fracture for a Spherical Characterization of the Rock Matrix

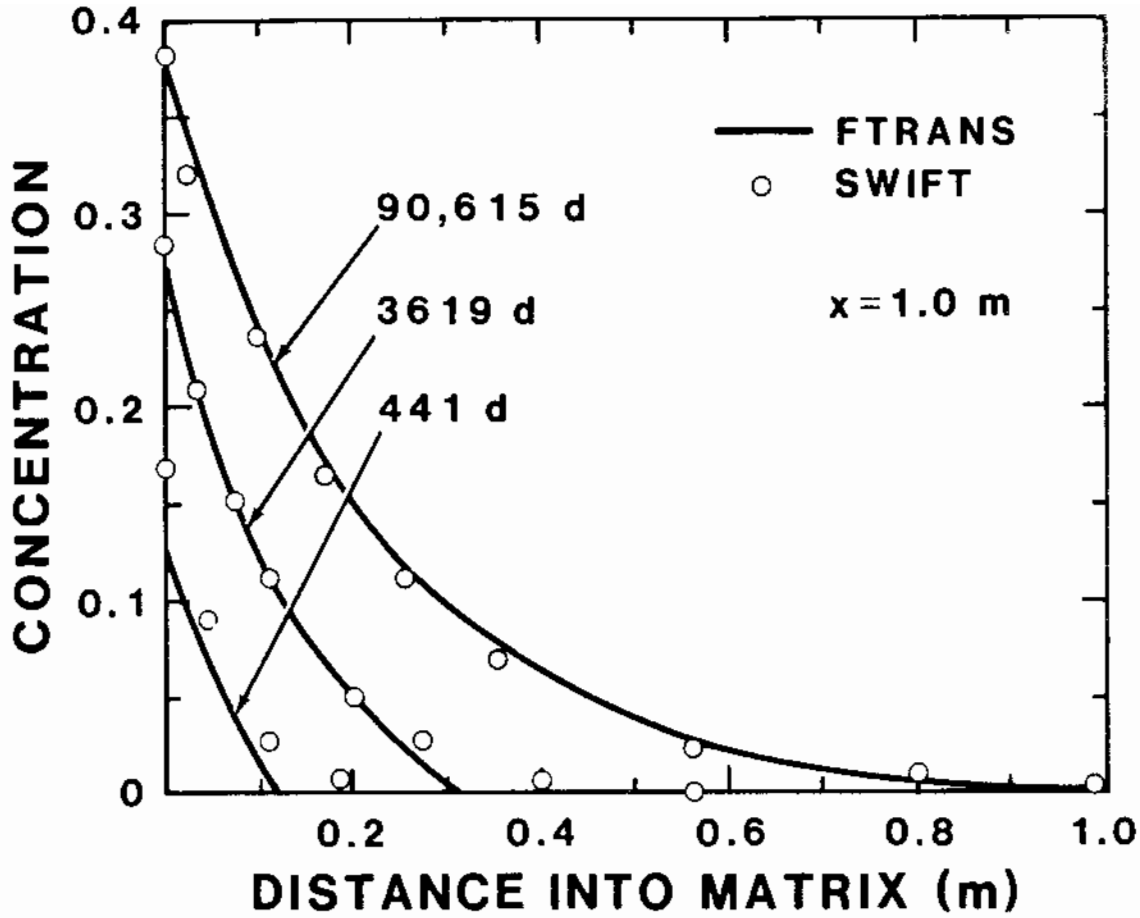

Figure 2.2-4. Radionuclide Concentrations Within the Rock Matrix for a Spherical Characterization of the Rock Matrix

2.3 PROBLEM 3. TRANSPORT OF A RADIONUCLIDE CHAIN IN FRACTURED POROUS MEDIA

2.3.1 Objective

The objective of Problem 3 is to illustrate the coupled effects of fracture/matrix transport and chain decay.

2.3.2 Description of the Problem

Problem Statement. Assume that radionuclides are buried in fractured media. The fractured media consist of parallel horizontal fractures of width 2d and separations 2a as illustrated in Figure 2.3-1. The media are laterally infinite, but confined to a vertical thickness $b = \Delta z$, by impermeable beds. The radionuclides are leached from a source for a duration, T_2. They are subsequently transported laterally in a one-dimensional flow field. Convection and dispersion occur within the fractures while diffusion and sorption occur within the rock matrix. The rock matrix is characterized by a set of one-dimensional prismatic units. This problem is similar to the problem performed for fractured porous media in the INTRACOIN (1983) report.

Transport Equations. Transport within the fractures for radionuclide r is given by the equation

$$- \frac{\partial}{\partial x} (\rho C_r u) + \frac{\partial}{\partial x} \left(\rho D \frac{\partial C_r}{\partial x} \right) - \Gamma_r \qquad (2.3\text{-}1)$$

$$+ k_{r,r-1} \lambda_{r-1} K_{r-1} \phi \rho C_{r-1} - \lambda_r K_r \phi \rho C_r = \frac{\partial}{\partial t} (K_r \phi \rho C_r)$$

and transport within the rock matrix is governed by

$$\frac{\partial}{\partial s} \left(\rho' D'_m \frac{\partial C'_r}{\partial s} \right) + \Gamma_r \qquad (2.3\text{-}2)$$

$$+ k_{r,r-1} \lambda_{r-1} K'_{r-1} \phi' \rho' C'_{r-1} - \lambda_r K'_r \phi' \rho' C'_r = \frac{\partial}{\partial t} (K'_r \phi' \rho' C'_r) \quad .$$

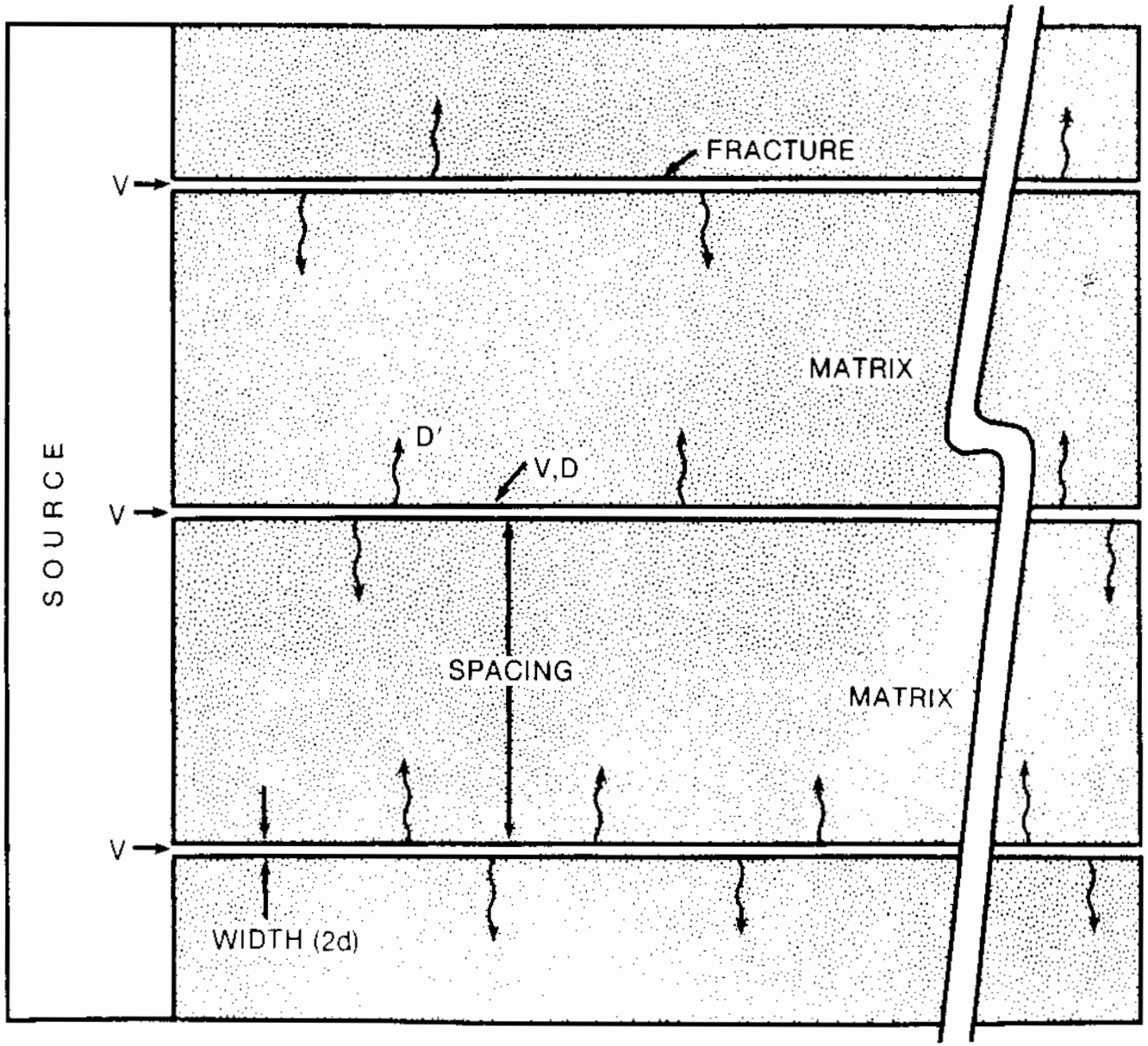

Figure 2.3-1. Problem 3. Schematic of Transport Within the Fracture and Diffusion Within the Matrix

The continuous flux at the fracture/matrix interface gives

$$\Gamma_r = A_V \rho' D'_m \left. \frac{\partial C'_r}{\partial s} \right|_{s=0} \qquad (2.3\text{-}3)$$

Initial/Boundary Conditions. Within the rock matrix, the concentration is initially zero:

$$C'_r(x,s,0) = 0 \qquad (2.3\text{-}4a)$$

the no-flux condition at the symmetry boundary is

$$\left. \frac{\partial C'_r}{\partial s} \right|_{s=a} = 0 \qquad (2.3\text{-}4b)$$

and fracture and matrix concentrations are identical at the fracture/matrix interface

$$C'_r(x,0,t) = C_r(x,t) \quad . \qquad (2.3\text{-}4c)$$

Within the fractures, the initial concentration is zero:

$$C_r(x,0) = 0 \qquad (2.3\text{-}5)$$

and the outlet boundary is held at this initial concentration.

Source Specification. At $x = 0$, the inlet boundary condition for the fractures must take into account both decay/production processes within the inventory and leaching of the inventory. To do this, the time-dependent source concentrations $\tilde{C}_r$ are defined by the Bateman equations:

$$\frac{d\tilde{C}_r}{dt} = k_{r,r-1}\lambda_{r-1}\tilde{C}_{r-1} - \lambda_r\tilde{C}_r \qquad (2.3\text{-}6a)$$

with initial conditions

$$\tilde{C}_r(t=0) = I_r/UT \quad . \qquad (2.3\text{-}6b)$$

The inlet boundary condition is expressed in terms of these source concentrations:

$$uC_r - D_r \frac{\partial C_r}{\partial x} = u\tilde{C}_r \quad , \quad x = 0 \quad . \qquad (2.3\text{-}7)$$

Additional Parameters. The geometry, the leaching process, and the transport process are characterized by the parameter values listed in Table 2.3-1. Radionuclide-dependent processes are determined by the parameters given in Table 2.3-2.

2.3.3 Numerical Simulation

Discussion of Code Input. Within the input-data listing of Figure 2.3-2, two items are selected for emphasis in this section. In contrast to Problems 1 and 2, the velocity is established by specifying the parameters that control the velocity calculations, especially the boundary pressures. The equation for the velocity is:

$$v = [K/\rho(g/g_c)\Phi](p_o - p_l)/L = 500 \text{ m/yr} \qquad (2.3\text{-}8)$$

where p_o and p_l are the pressures at the inlet and outlet respectively. In this equation, the porosity of the global system

$$\Phi = d/(a+d) = 1.99996 \times 10^{-5} \quad , \quad \text{R1-20} \qquad (2.3\ 9a)$$

is fixed in the input (Table 2.3-1). The system length

$$L = 2{,}500 \text{ m} \quad , \quad \text{R1-17} \qquad (2.3\text{-}9b)$$

(the sum of all increments in Card R1-17) is taken to be large compared to the observation length (500 m) in order to simulate semi-infinite media. The gravitational acceleration constant ($g = 9.81$ m/s^2) is fixed in the code.

All other parameters in Equation (2.3-8) are specified to yield the desired interstitial velocity:

Table 2.3-1

Problem 3. Data

Parameter	Symbol	Value
Observation Length	L_l	500 m
Aquifer Thickness	b	5.0 m
Fracture Aperture	$2d$	1.0×10^{-4} m
Fracture Spacing	$2a$	5.0 m
Fracture Porosity	ϕ	2.0×10^{-5}
Fracture Velocity	v	500 m/y
Fracture Dispersity	α_L	50 m
Matrix Porosity	ϕ'	5.0×10^{-3}
Rock Density	ρ_R	2700 kg/m^3
Matrix Diffusivity	D_m'	1.0×10^{-12} m^2/s
Leach Duration	T_2	10^5 y

Table 2.3-2

Nuclide Inventory (I_2) and Matrix* Retardation (R_3).

Number	Isotope	Inventory (Ci)	Inventory (kg)	Half-Life** τ(y)	Retardation K_v	Distribution Coefficient*** k_d (m^3/kg)	Specific Activity A_m (Ci/kg)
1	^{245}Cm	0.7	4.074×10^{-3}	8.500×10^{3}	570	0.211	171.8
2	^{237}Np	1.0	1.418	2.140×10^{6}	80	2.96×10^{-2}	0.7055
3	^{233}U	0.004	4.147×10^{-4}	1.592×10^{6}	30	1.11×10^{-2}	9.646

* No sorption occurs within the fracture.

** The corresponding decay constant is given by $\lambda = \ell n(2)/\tau$.

*** The two sorption parameters are related via $K_v = \rho_R k_d$.

```
PROBLEM NO. 3,   INTRACOIN LEVEL 1, CASE 5, I2,R3,B2,P2,T2,E1,L1          M-1-1
03/86,  ONE-D TRANSPORT IN FRACTURED MEDIA WITH CHAIN DECAY               M-1-2
    4     0     0     0     0     0     0     1     1                     M-2
  126     1     1     1     3     1     1    -1     0     2     0     1     1    0M-3-1
    1     2     1     1                                                   M-3-2
245AM 245             1     0     0     8.5E3                             RO-1-1
237NP 237             2     1     0     2.14E6                            RO-1-1
    1         1  0                                                        RO-1-2
233 U 233             3     1     0   1.592E5                             RO-1-1
    2         1  0                                                        RO-1-2
        0.0         0.0         0.0                                       RO-2-1
        1.0         1.0         1.0                                       RO-2-2
    6                                                                     ROD-1
   25                                                                     ROD-2
    1  126     1     1     1     1     1     0                           ROD-3
                                                                          ROD-3-BLN
        0.0         0.0         0.0    4186.0         1.0                R1-1
        0.0         0.0         0.0       0.0        50.0      0.0  1.0E-20R1-2
     2700.0         0.0        20.0    1000.0      1000.0                 R1-3
    2     2     2     2                                                   R1-6
       20.0       0.001       20.0       0.001                           R1-7
       0.20       0.001       0.80       0.001                           R1-8
      100.0       0.001      200.0       0.001                           R1-9
      100.0       0.001      200.0       0.001                           R1-10
        0.0        20.0                                                  R1-11
      100.0        20.0                                                  R1-11
    0     0                                                               R1-12
       20.0         0.0         0.0         0.0                          R1-16
        1.0         2.0         3.0       98*5.0        9.0      10.0      20.0
       30.0        40.0        50.0        60.0       80.0  16*100.0     105.0
        1.0
    5.0001
1.99996E-51.99996E-51.99996E-51.99996E-5 0.0        0.0         0.0       R1-20
                                                                          R1-26-BLN
    4     0                                                               R1-27
    1     1     1     1     1     1                                       R1-28-1
        1.0 388.44495         20.0          0.0                           R1-28-2
  126   126     1     1     1     1                                       R1-28-3
        2.0         0.0         20.0          0.0                       R1-28-4
                                                                          R1-28-BLN
                                                                          R1-33-BLN
        0.0                                                               R1D-1
  1.00E-12          0.0   5.00E-03          0.0         0.0       0.0     1.0R1D-2-1
    1     1           2.5   1.00E-3           0.0                         R1D-2-2
                                                                          R1D-3-BLN
   2.11E-1     2.96E-2     1.11E-2                                        R1D-4
                                                                          R1D-5-BLN
    0     0     0                                                         I-1
        0.0                                                               R1A-2
    0                                                                     R1A-3
```

Figure 2.3-2. Problem 3. Listing of SWIFT II Input Data

```
       0.0         0.0  0.199996          0.0                                  R1A-4
       1.0         1.0       1.0                                               R1A-5
     1    1     1    1     1    1                                               R1A-6
       0.0                                                                     R1A-7
CM 245       4.0743E-3                                                         R1A-8
NP 237           1.4175                                                        R1A-8
 U 233       4.1470E-4                                                         R1A-8
      10.0         10.0       10.0                                            R1A-9
  102     1     1                                                             N-1
                                                                              N-1-BLN
    0     0     1     0     0     0     0     0     0     0                   R2-1
    1         0.5                                                             R2-2
       1.0         1.0
    1    -1     1    -1    -1     1   111     0 0000     0   11    -1   211   11R2-13
    0     0     0     0     2     0     0     0     0     0                   R2-1
 3.1536E12          0 0                                                      R2-13.5
6.3072 E11 15.768E09
    1    -1    -1    -1     1    -1   211     1 0000     0   00     1   211   00R2-13
    0     0     0     0     0     0     0     0     0     0                   R2-1
25.2288E11 15.768E09
    1    -1    -1    -1     1    -1   211     1 0000     0   00     1   211   00R2-13
    0     0     0     0     0     0     0     0     0                         R2-1
4.7304 E12 3.1536E10
    1    -1    -1    -1     1    -1   211     1 0000     0   00     1   211   00R2-13
    0     0     0     0     0     0     0     0     0                         R2-1
5.67648E12 3.1536E10
    1    -1    -1    -1     1    -1   211     1 0000     0   00     1   211   00R2-13
    0     0     0     1     0     0     0     0     0                         R2-1-END
```

Figure 2.3-2. Problem 3. Listing of SWIFT II Input Data (Continued)

$$\rho = 1000 \text{ kg/m}^3 \quad , \quad \text{R1-3} \tag{2.3-10a}$$

$$K = 1.99996 \times 10^{-5} \text{ m/s} \quad , \quad \text{R1-20} \tag{2.3-10b}$$

$$p_o = 388.44495 \text{ Pa} \quad , \quad \text{R1-28-2} \tag{2.3-10c}$$

and

$$p_1 = 0 \quad , \quad \text{R1-28-2} \tag{2.3-10d}$$

The inlet boundary condition at grid Block 1 is specified as the source in Card R1A-6. This block is only 1 m long (Card R1-17). Therefore, it should be an acceptable approximation to the boundary condition of Equation (2.3-7), prescribed for an infinitesimal increment.

The source rate is specified in the code by the equation

$$R_{wr} = -m_r(t)\rho_w/t_a \tag{2.3-11}$$

(Section 3.4 of Theory and Implementation) where

R_{wr} = source rate of radionuclide r [kg/m^3(bulk)/s],

m_r = density of radionuclide r in the waste [kg/m^3(waste)],

ρ_w = volumetric fraction of wastes [m^3(waste)/m^3(bulk)],

$t_a = T_2$ = leach duration [s] .

Quantities t_a, $m_r(0)$, and ρ_w must be specified in the input. The waste inventory is assumed to occupy one m^3 so that

$$\rho_w = 1/\Delta x_1 \Delta y \Delta z = 0.199996 \quad , \quad \text{R1A-4} \tag{2.3-12}$$

where $\Delta x_1 = 1$ m, $\Delta y = 1$ m and $\Delta z = 5.0001$ m are specified in Cards R1-17, R1-18, and R1-19, respectively. Also the initial densities $m_r(0)$ have the same values as the radionuclide inventories I_r (Table 2.3-2), and the code computes for the Bateman decay (Equation 2.3-6a).

Code Output. The radionuclide concentrations in each grid block within the fracture and within the matrix are

presented on the microfiche in the back cover of this document. The concentrations, expressed as kg of radio nuclides/kg of water, are printed for four selected time intervals. The gridding of the fracture/matrix system is shown in Figure 2.3-3 and is also printed on the microfiche output listing.

To provide a check on the calculation of concentrations, four material-balance summaries are printed at each time interval. Two of them, one for unleached components and one for leached but undissolved components, pertain to the source block. The other two, one for dissolved and sorbed material in the fracture and one for such material residing in the rock matrix, pertain to the system as a whole. These tables list the amount of each component within a particular phase or subsystem and provide a mass balance quotient. Ideally, these quotients should equal unity. The categories used in these tables are defined in Table 2.3-3.

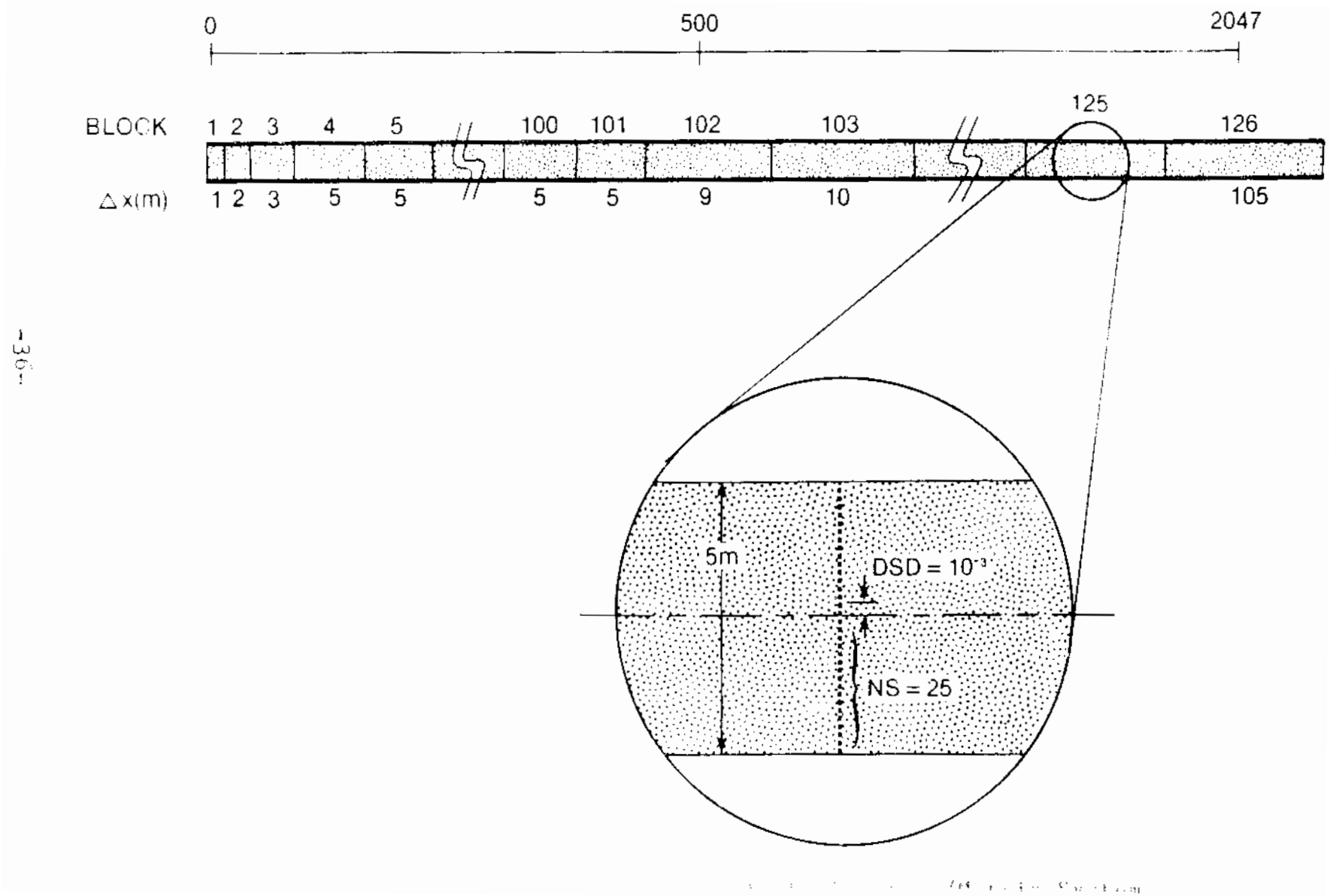
0
500
2047
BLOCK
1 2 3 4 5 100 101 102 103 125 126
Δx(m)
1 2 3 5 5 5 5 9 10 105
5m
DSD = 10⁻³
NS = 25

presented on the microfiche in the back cover of this document. The concentrations, expressed as kg of radio nuclides/kg of water, are printed for four selected time intervals. The gridding of the fracture/matrix system is shown in Figure 2.3-3 and is also printed on the microfiche output listing.

To provide a check on the calculation of concentrations, four material-balance summaries are printed at each time interval. Two of them, one for unleached components and one for leached but undissolved components, pertain to the source block. The other two, one for dissolved and sorbed material in the fracture and one for such material residing in the rock matrix, pertain to the system as a whole. These tables list the amount of each component within a particular phase or subsystem and provide a mass balance quotient. Ideally, these quotients should equal unity. The categories used in these tables are defined in Table 2.3-3.

Table 2.3-3

Material-Balance Summaries[1]

	Unleached[2]	Leached but Undissolved[2,3]	(Fracture) Dissolved and Sorbed	Matrix Dissolved and sorbed
In Place	Mass unleached from radioactive-waste storage	Mass leached from storage, but, as yet, undissolved	Total mass in transport within fracture	Total mass in transport within matrix
Sources	---	Gain from unleached phase	Gain from leached-but-undissolved phase and from specified sources	Gain of mass transported from fracture to matrix subsystem
Sinks	Loss to leached-but-undissolved phase	Loss to (fracture) dissolved and sorbed phase	Loss to withdrawal wells	Loss of mass transported from matrix to fracture subsystem
Generation	Mass generated by radioactive decay of parent(s) within the inventory	Mass generated by radioactive decay of parent(s) within the phase	Mass generated by radioactive decay of parent(s) within the fracture	Mass generated by radioactive decay of parent(s) within matrix
Decay	Loss through radioactive decay of initial inventory	Loss through radioactive decay within the phase	Loss through radioactive decay within the fracture	Loss through radioactive decay within matrix
E-Flux	---	---	Loss at boundary-discharge locations	---

1 All entries are masses accumulated over time.
2 Refer to source block only.
3 Undissolved due to solubility limitation.

3. FLUID FLOW THROUGH DUAL-POROSITY MEDIA

3.1 PROBLEM 4. ANALYSIS OF WELL-TEST DATA FOR A DOLOMITE FORMATION [PAHWA AND BAXLEY, 1980]

3.1.1 Objective

The objective of Problem 4 is to simulate a slug-injection test in dual porosity media.

3.1.2 Description of the Problem

Background. A number of slug and recovery tests were conducted by Sandia National Laboratories and by the U.S. Geological Survey [Mercer and Orr, 1979; Dennehy and Davis, 1981] during the site-characterization work for the Waste-Isolation Pilot Plant (WIPP) [Powers et al., 1978]. Two formations of particular interest were the Culebra and Magenta dolomite members of the Rustler unit, both of which are significant water-bearing rocks lying above the Salado salt layer. These tests were analyzed by Dennehy and Davis (1981) using an analytical model and, because many of the tests exhibited an anomalously high flow rate at small values of time, they were analyzed also by Pahwa and Baxley (1980) using a dual-porosity implementation of their numerical code.

In the SWIFT Self-Teaching Curriculum, Problem 11 [Finley and Reeves, 1981], the H2A test (Figure 3.1-1) of the Magenta member was chosen, and the conceptual model of Pahwa and Baxley (1980) was used. This model assumes that in addition to the primary porosity (which may itself represent connected fractures extending throughout the dolomite) there are secondary-porosity fractures that extend radially outward an average distance of 2000 ft (Figure 3.1-2a). These fractures are assumed to cause the small-time flow response. As in the work of Pahwa and Baxley (1980), heterogeneity was used in Problem 11 to characterize the secondary porosity.

Problem Statement. In this problem, a different conceptual model is used. The secondary porosity is assumed to be provided by stress-relief fracturing that extends about one foot radially around the wellbore (see Figure 3.1-2b). The dual-porosity approach of the SWIFT II code is used to simulate the reported data.

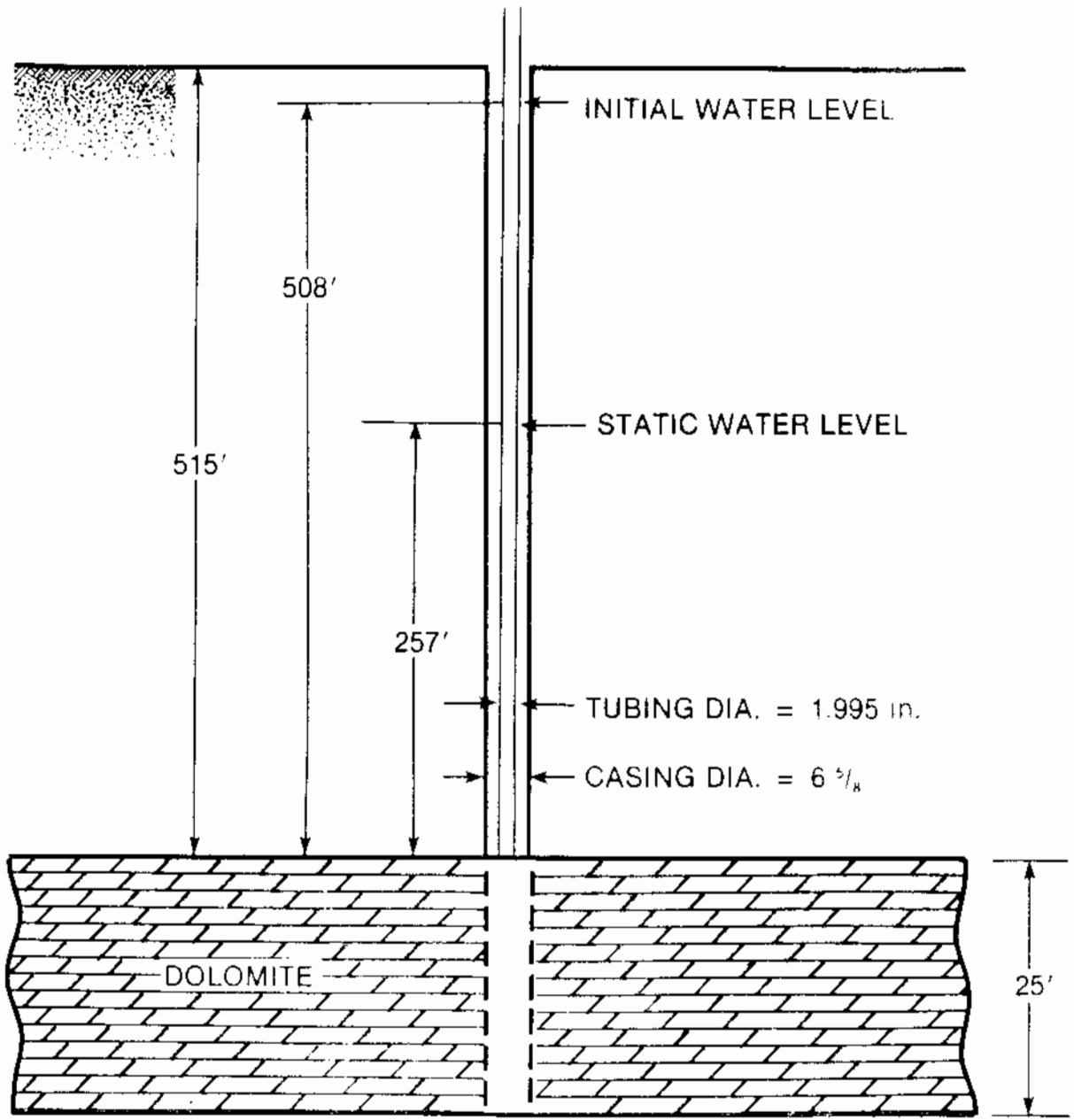

Figure 3.1-1. Problem 4. Diagram of Well H2A Within the Magenta Dolomite Formation

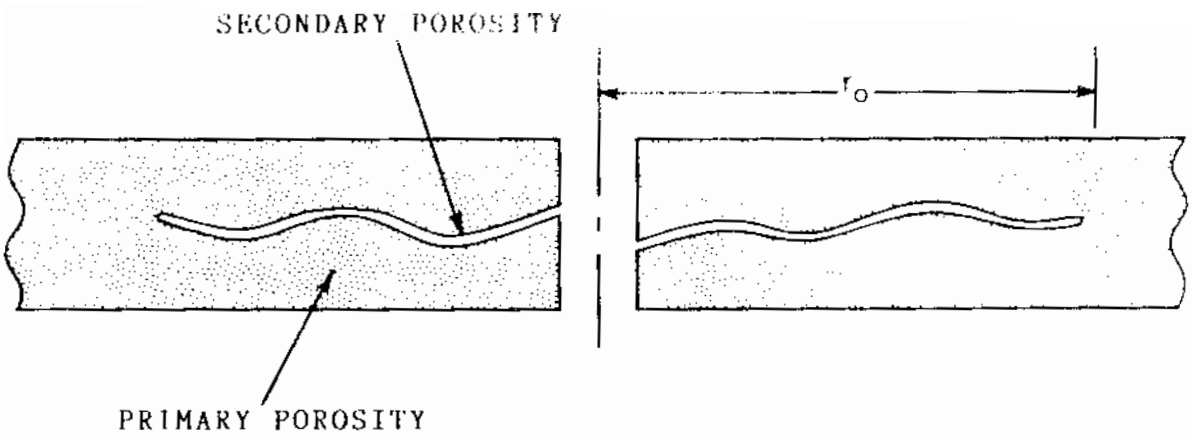

(a) Partially Penetrating Fracture(s).

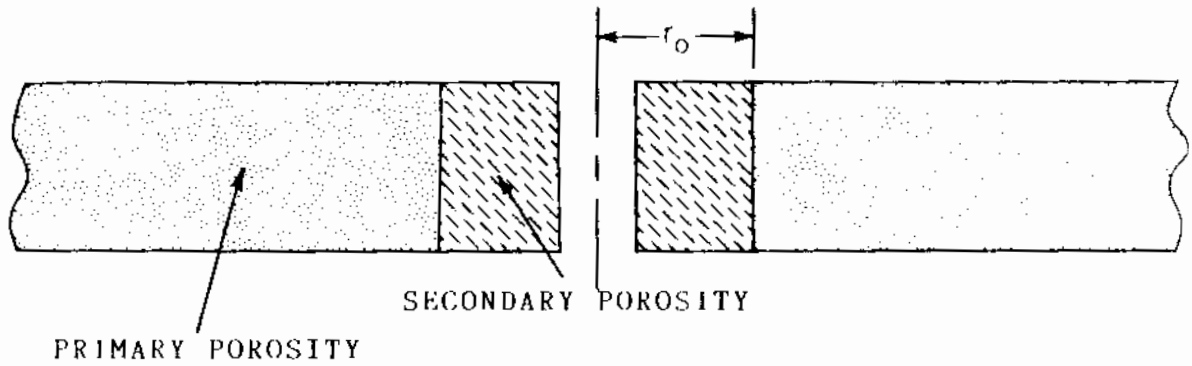

(b) Stress-Relief Fractures

Figure 3.1-2. Conceptual Models for the Secondary Fracture Porosity

Flow Equations. Within the primary porosity (the global blocks), the flow is described by

$$T \frac{1}{r} \frac{\partial}{\partial r} \left(r \frac{\partial \bar{s}}{\partial r}\right) - b\Gamma_w = S \frac{\partial \bar{s}}{\partial t} \quad , \quad r_w \leq r \leq \infty \qquad (3.1\text{-}1)$$

and, within the secondary porosity (the local blocks) by

$$K' \frac{\partial^2 \bar{s}'}{\partial s^2} + \Gamma_w = S'_s \frac{\partial \bar{s}'}{\partial t} \quad , \quad 0 < s < a, \; r_w < r \leq r_o \qquad (3.1\text{-}2)$$

where a is the average length of the connected secondary fracturing and r_o is the maximum extent of the stress-relief fracturing surrounding the wellbore (radius, r_w). The coupling between primary and secondary porosity is provided by the relation

$$\Gamma_w = - A_v K' \left. \frac{\partial \bar{s}'}{\partial s} \right|_{s=0} \qquad (3.1\text{-}3)$$

Initial/Boundary Conditions. Within the secondary porosity, the initial drawdown is zero

$$\bar{s}'(r,s,0) = 0 \qquad (3.1\text{-}4a)$$

the drawdowns are set equal at the interfaces

$$\bar{s}'(r,0,t) = \bar{s}(r,t) \qquad (3.1\text{-}4b)$$

and a no-flow boundary is the default condition prescribed at the edge of the local blocks

$$\left. \frac{\partial \bar{s}'}{\partial s} \right|_{s=0} = 0 \qquad (3.1\text{-}4c)$$

Within the primary porosity, the initial drawdown is zero

$$\bar{s}(r,0) = 0 \qquad (3.1\text{-}5a)$$

and the water-level at the wellbore radius r_w is set equal to the water-level in the well:

$$\bar{s}(r_w,t) = s_o(t) \quad . \tag{3.1-5b}$$

Input/Output Specifications. The SWIFT II code solves for pressure. Thus, in the above equations, drawdown is replaced by pressure as the dependent variable:

$$s = p_o - p \tag{3.1-6}$$

where p_o is the initial pressure. Also the storativity and transmissivities are replaced by the equivalent expressions:

$$S = \rho(g/g_c)\phi(c_w+c_R)b \tag{3.1-7a}$$

$$T = Kb \tag{3.1-7b}$$

and

$$S'_s = \rho(g/g_c)\phi'(c_w+c'_R) \quad . \tag{3.1-7c}$$

Problem data are listed in Table 3.1-1. The primary porosity is from Pahwa and Baxley (1980). The secondary porosity was obtained by model calibration. The remainder of the data, time-dependent height of the water level within the wellbore, is listed in Table 3.1-2. Pahwa and Baxley (1980) treated the wellbore storage implicitly and the water level and the injected flow rates were calculated. In this simulation the measured water levels are prescribed as input data, and the injected flow rates are calculated.

Table 3.1-1

Problem 4. Data

Parameter	Symbol	Value
Density of Water	ρ	62.4 lbm/ft^3
Aquifer Thickness	b	25.0 ft
Compressibility of Water	c_w	3.0 x 10^{-6} psi^{-1}
Primary-Porosity Media:		
Porosity	Φ	0.10
Compressibility of Rock	c_R	4.0 x 10^{-6} psi^{-1}
Hydraulic Conductivity	K	2.0 x 10^{-4} ft/d
Storativity	S	7.58 x 10^{-6}
Transmissivity	T	0.005 ft^2/d
Secondary-Porosity Media:		
Porosity	Φ'	0.10
Compressibility of Rock	c_R'	4.0 x 10^{-5} psi^{-1}
Hydraulic Conductivity	K'	200.0 ft/d
Length	a	25.0 ft
Specific Storativity	S_S'	1.86 x10^{-6} ft^{-1}

Table 3.1-2

Measured Bottom-Hole Pressure and Calculated Water Level

Time Interval (days)	Water Level Height (ft)	Bottom-Hole Pressure (psi)
10^{-4} - 10^{-2}	505	219
10^{-2} - 10^{-1}	496	215
0.1 - 0.2	485	210
0.2 - 0.5	468	203
0.5 - 0.8	450	195
0.8 - 1.0	434	188
1.0 - 1.5	415	180
1.5 - 2.0	392	170
2.0 - 2.5	374	162
2.5 - 3.0	360	156

3.1.3 Numerical Simulation

Code Input. In this problem a radial coordinate system is employed. The inner boundary is a well of radius r_w = 0.276 ft (Card R1-22, Figure 3.1-3). This well communicates with the aquifer through a wellskin, which represents a zone of modified hydraulic properties. For the SWIFT II code, the wellskin is assumed to have no storage and a hydraulic-conduction property that is characterized by a well index (Reeves et al., 1986a, Section 4.1):

$$WI_o = 2\pi K_s \Delta z / \ell n(r_1/r_w) \qquad (3.1\text{-}8)$$

where the quantities r_1 = 1.0 ft, the position of the first global node within the mesh, and Δz = 25 ft are listed in Cards R1-22 and R1-23.

The wellskin is represented by a one-dimensional unit (a local block) attached to the first grid block (Card ROD 3). This unit has storage and a relatively large hydraulic conductivity. Thus, the well index (Card R2-7.2) has been superseded by this one-dimensional unit.

The outer boundary is chosen as

$$r_e = 2000 \text{ ft}, \qquad (3.1\text{-}9a)$$

which is beyond the limits of the pressure response imposed by the well:

$$\tilde{r}_e = (Tt_{max}/S)^{1/2} = 100 \text{ ft} \quad . \qquad (3.1\text{-}9b)$$

At this boundary, an analytic solution (Carter and Tracy, 1960) is used to simulate an infinite aquifer. These data appear on Cards R1-27 through R1-33.

Results. The simulated and measured flow rates as a function of time are shown in Figure 3.1-4. These rates agree reasonably well.

Code Output. The table entitled "Radial Grid Block Data", (see output listing in microfiche) lists radial distances to nodal points and grid-block boundaries. These radii have been internally generated (R1 = 0 in Card R1-22) assuming an equal ratio:

```
PROBLEM NO. 4, SWIFT II EXAMPLE, ENGLISH UNITS, 03/86,                  M-1-1
INTERPRETATION OF WELL TEST DATA FOR A DOLOMITE FORMATION, NEW MEXICO M-1-2
   1     0     0     0     0     0     0     0     0                    M-2
  50     1     1     3     0     1     1     2     0     1     0     0     0M-3-1
   0     1     1     1                                                  M-3-2
   0                                                                    ROD-1
   8                                                                    ROD-2
   1     1     1     1     1     1     1     0                          ROD-3
                                                                        ROD-3-BLN
.000003      000004          0.0          1.0          1.0             R1-1
     1.0          1.0          1.0          1.0          1.0      0.0      .0001R1-2
   120.         100.          70.         62.4         62.4             R1-3
   0     1     0     2                                                  R1-6
    70.          1.0          70.          1.0                        R1-7
   100.          1.0                                                   R1-9
     0.0         70.0                                                  R1-11
  1000.0         70.0                                                  R1-11
   0     0                                                            R1-12
    70.0        111.5         514.6        514.6                       R1-16
   0.276          1.00        2000.        514.6                       R1-22
    25.         .0002         .0002         0.10                       R1-23
                                                                        R1-26-BLN
   3                                                                    R1-27
   1     0     1                                                        R1-29
   0.005          2.5         2000.         360.                       R1-31
                                                                        R1-33-BLN
.00004                                                                  R1D-1
  .0003          0.0           0.1   2.00E+02          0.0      0.0      0.0R1D-2-1
   1     1         25.0          2.0          0.0                      R1D-2-2
                                                                        R1D-3-BLN
                                                                        R1D-5-BLN
   0     0     0                                                        I-1
     0.0                                                                R1A-2
   2     1     1     0     0     0     0     1     0                    R2-1
   1          0.5                                                       R2-2
   1                                                                    R2-4
   1     -9999.                                                         R2-6
                                                                        R2-6-BLN
   1     1     1     1     1    -3                                      R2-7-1
     .10         220.0         70.0          0.0                      R2-7-2
                                                                        R2-7-BLN
   1     1     1                                                        R2-11
0.0001       0.0001
   1     1     1     1                                                  R2-13
   0     1     0     0     0     0     0     0                          R2-1
   1     1     1     1     1    -3                                      R2-7-1
     .10         219.0         70.0          0.0                      R2-7-2
                                                                        R2-7-BLN
    0.01          0.0           0.0          0.0          3.0      0.0      0.5    0.0001
  -1    -1    -1    -1    -1    -1   011     0 0000     0     0     1  011     0R2-13
```

Figure 3.1-3. Problem 4. Listing of SWIFT II Input Data

```
  0     1     0     0     0     0     0     0                                                  R2-1
  1     1     1     1     1    -3                                                              R2-7-1
      .10      215.0        70.0           0.0                                               R2-7-2
                                                                                             R2-7-BLN
    0.30          0.0          0.0          0.0          3.0          0.0          0.5     0.0001
  1     1     1     1     1     1   011     0 0000     0     0     1   011     0R2-13
  0     1     0     0     0     0     0     0                                                  R2-1
  1     1     1     1     1    -3                                                              R2-7-1
      .10      209.5        70.0           0.0                                               R2-7-2
                                                                                             R2-7-BLN
    0.20          0.0          0.0          0.0          3.0          0.0          0.5     0.0001
  1    -1     1    -1    -1     1   011     0 0000     0     0     1   011     0R2-13
  0     1     0     0     0     0     0     0                                                  R2-1
  1     1     1     1     1    -3                                                              R2-7-1
      .10      203.9        70.0           0.0                                               R2-7-2
                                                                                             R2-7-BLN
    0.50          0.0          0.0          0.0          3.0          0.0          0.5     0.0001
 -1    -1    -1    -1    -1    -1   011     0 0000     0     0     1   011     0R2-13
  0     1     0     0     0     0     0     0                                                  R2-1
  1     1     1     1     1    -3                                                              R2-7-1
      .10      196.0        70.0           0.0                                               R2-7-2
                                                                                             R2-7-BLN
    0.80          0.0          0.0          0.0          3.0          0.0          0.5     0.0001
 -1    -1    -1    -1    -1    -1   011     0 0000     0     0     1   011     0R2-13
  0     1     0     0     0     0     0     0                                                  R2-1
  1     1     1     1     1    -3                                                              R2-7-1
      .10      190.0        70.0           0.0                                               R2-7-2
                                                                                             R2-7-BLN
    1.00          0.0          0.0          0.0          3.0          0.0          0.5     0.0001
  1     1     1     1     1     1   011     0 0000     0     0     1   011     0R2-13
  0     1     0     0     0     0     0     0                                                  R2-1
  1     1     1     1     1    -3                                                              R2-7-1
      .10      184.0        70.0           0.0                                               R2-7-2
                                                                                             R2-7-BLN
    1.25          0.0          0.0          0.0          3.0          0.0          0.5     0.0001
 -1    -1    -1    -1    -1    -1   011     0 0000     0     0     1   011     0R2-13
  0     1     0     0     0     0     0     0                                                  R2-1
  1     1     1     1     1    -3                                                              R2-7-1
      .10      179.5        70.0           0.0                                               R2-7-2
                                                                                             R2-7-BLN
    1.50          0.0          0.0          0.0          3.0          0.0          0.5     0.0001
 -1    -1    -1    -1    -1    -1   011     0 0000     0     0     1   011     0R2-13
  0     1     0     0     0     0     0     0                                                  R2-1
  1     1     1     1     1    -3                                                              R2-7-1
      .10      175.0        70.0           0.0                                               R2-7-2
                                                                                             R2-7-BLN
    1.75          0.0          0.0          0.0          3.0          0.0          0.5     0.0001
 -1    -1    -1    -1    -1    -1   011     0 0000     0     0     1   011     0R2-13
  0     1     0     0     0     0     0     0                                                  R2-1
  1     1     1     1     1    -3                                                              R2-7-1
```

Figure 3.1-3. Problem 4. Listing of SWIFT II Input Data (Continued)

```
      .10      171.0       70.0        0.0                                    R2-7-2
                                                                              R2-7-BLN
     2.00        0.0        0.0        0.0        3.0        0.0        0.5     0.0001
 -1   -1   -1   -1   -1   -1   011     0 0000     0     0     1   011     0R2-13
  0    1    0    0    0    0    0      0                                     R2-1
  1    1    1    1    1   -3                                               R2-7-1
      10      164.0       70.0        0.0                                    R2-7-2
                                                                              R2-7-BLN
     2.25        0.0        0.0        0.0        3.0        0.0        0.5     0.0001
  1   -1   -1    1   -1   -1   011     0 0000     0     0     1   011     0R2-13
  0    1    0    0    0    0    0      0                                     R2-1
  1    1    1    1    1   -3                                               R2-7-1
      .10      164.0       70.0        0.0                                    R2-7-2
                                                                              R2-7-BLN
     2.50        0.0        0.0        0.0        3.0        0.0        0.5     0.0001
 -1   -1   -1   -1   -1   -1   011     0 0000     0     0     1   011     0R2-13
  0    1    0    0    0    0    0      0                                     R2-1
  1    1    1    1    1   -3                                               R2-7-1
      10      161.0       70.0        0.0                                    R2-7-2
                                                                              R2-7-BLN
     2.75        0.0        0.0        0.0        3.0        0.0        0.5     0.0001
 -1   -1   -1   -1   -1   -1   011     0 0000     0     0     1   011     0R2-13
  0    1    0    0    0    0    0      0                                     R2-1
  1    1    1    1    1   -3                                               R2-7-1
      .10      158.0       70.0        0.0                                    R2-7-2
                                                                              R2-7-BLN
     3.00        0.0        0.0        0.0        3.0        0.0        0.5     0.0001
  1    1    1    1    1    1   011     0 0000     0     0     1   011     0R2-13
  0    0    0    1    0    0    0      0    0                                R2-1-STOP
```

Figure 3.1-3. Problem 4. Listing of SWIFT II Input Data (Continued)

$$A = r_{i+1} / r_i \qquad (3.1\text{-}10a)$$

for neighboring nodal points. The ratio is

$$A^{NX-1/2} = RE/R1 \text{ or } A = 1.16597 \qquad (3.1\text{-}10b)$$

where NX = 50 (Card M-3-1), RE = 2000 ft (Card R1-22), and R1 = 1.0 ft (Card R1-22)

Another table, "Data for Carter-Tracy Water Influx Calculations", lists information used to determine the outer boundary condition. The use of this type of boundary condition assumes that the simulated aquifer continues to infinity as an aquifer with parameters Kb (KH) and ϕb (PHIH). The dimensionless pressure drop (PI) listed in the table is for the boundary $r = r_e$. This pressure results from a unit flow across this boundary. This pressure is then used to calculate a boundary flux in the relation

$$e_W = a_W(P_I) + b_W(P_I)\delta p \quad . \qquad (3.1\text{-}11)$$

This flux is in terms of the pressure change δp at $r = r_e$, which occurs during a given time step. Quantities a_W and b_W are functions of P_I and, therefore, also of time.

The tables entitled "Well Operation Summary", are printed at selected time steps and provide the desired results that are graphically presented in Figure 3.1-4.

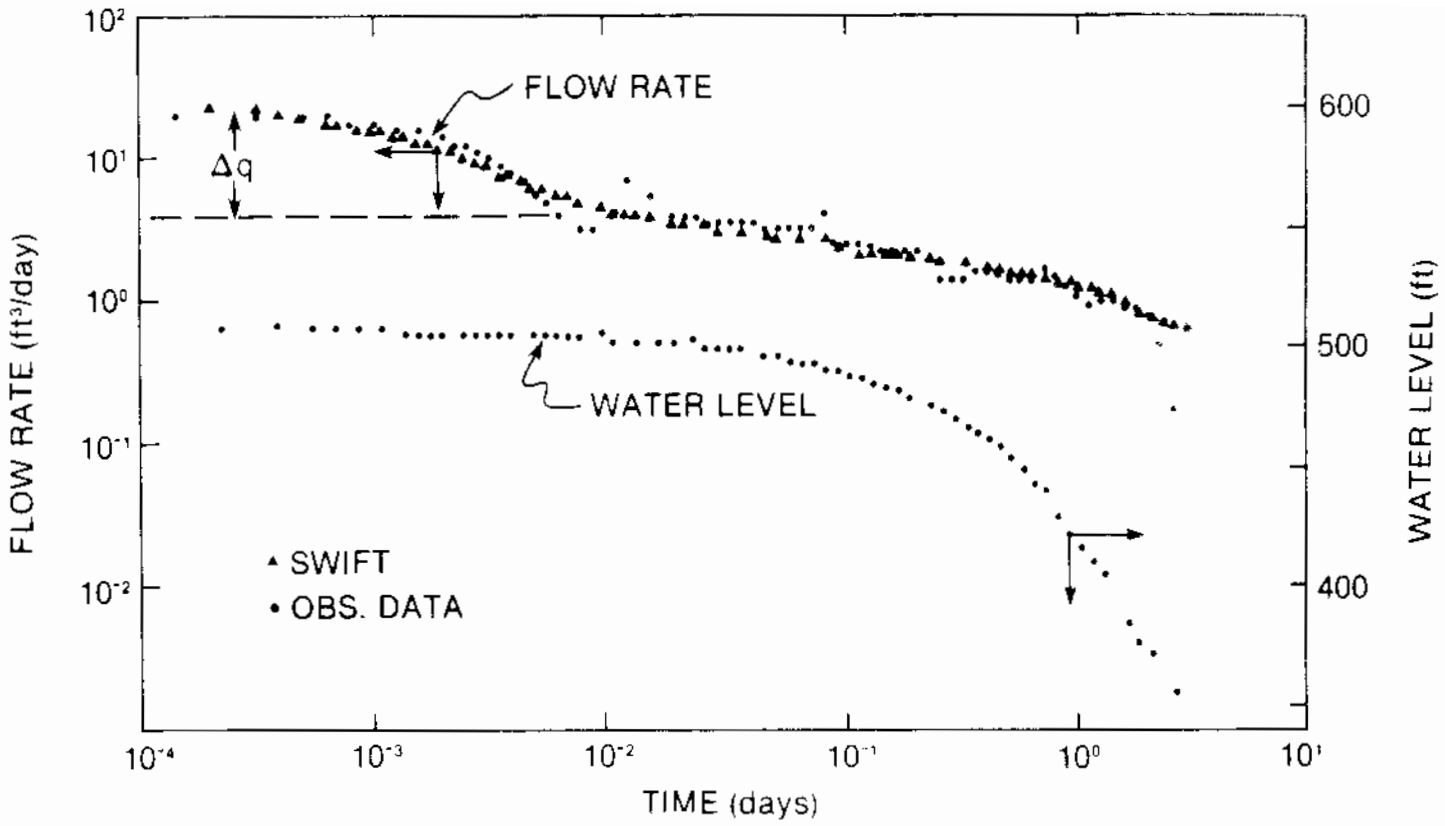

Figure 3.1-4. Flow Rate During H2A Slug Test

4. FLOW AND TRANSPORT THROUGH AN AQUIFER WITH CONFINING LAYERS

4.1 PROBLEM 5. DRAWDOWN IN A FULLY PENETRATING WELL IN A LEAKY AQUIFER [HANTUSH, 1960]

4.1.1 Objective

The objective of Problem 5 is to illustrate the use of the one-dimensional local units for simulating the effects of a leaking aquitard.

4.1.2 Problem Description

Problem Statement. A well penetrates completely an infinite aquifer and is pumped at a constant rate. The aquifer is bounded from below by an impermeable bed and from above by a confining bed (see Figure 4.1-1).

Flow Equations. The flow equation for the aquifer is given by

$$T \frac{1}{r} \frac{\partial}{\partial r} \left(r \frac{\partial \bar{s}}{\partial r}\right) - b\Gamma_w = S \frac{\partial \bar{s}}{\partial t} \qquad (4.1\text{-}1)$$

and for the confining bed, by

$$K' \frac{\partial^2 \bar{s}'}{\partial z^2} + \Gamma_w = S'_s \frac{\partial \bar{s}'}{\partial t} \quad . \qquad (4.1\text{-}2)$$

Only vertical flow is simulated in the confining bed. Continuity of flow across the interface between aquifer and aquitard results in:

$$\Gamma_w = A_V K' \left. \frac{\partial \bar{s}'}{\partial z} \right|_{z=0} \qquad (4.1\text{-}3)$$

where $A_V = 1/b$ is the interface area per unit of aquifer volume.

Initial/Boundary Conditions. For the aquifer and the confining bed the initial drawdown is zero:

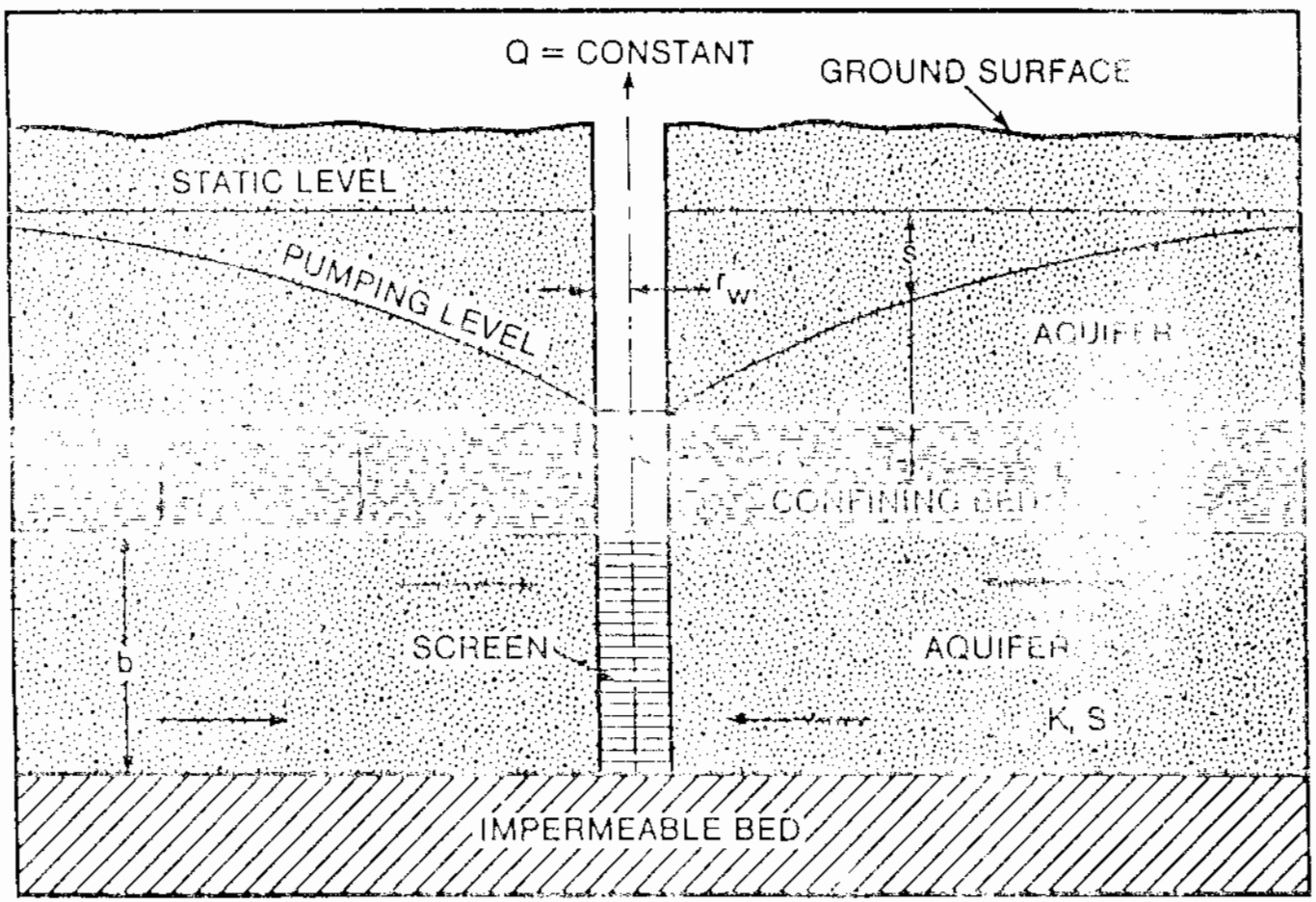

Figure 4.1-1. Problem 5. Diagram of a Fully Penetrating Constant-Discharge Well in a Leaky Aquifer

$$\bar{s}(r,0) = 0 \qquad (4.1\text{-}4a)$$

$$\bar{s}'(r,z,0) = 0 \qquad (4.1\text{-}4b)$$

and the aquifer discharge at the origin is:

$$\lim_{r \to 0} \left(r \frac{\partial \bar{s}}{\partial r} \right) = \frac{Q}{2\pi T} \qquad (4.1\text{-}4c)$$

and the interface condition is:

$$\bar{s}'(r,0,t) = \bar{s}(r,t) \qquad (4.1\text{-}5a)$$

where z is positive downward from the aquifer-aquitard interface. A constant hydraulic head is assumed at the upper boundary of the aquitard;

$$\bar{s}'(r,-b',t) = 0 \quad . \qquad (4.1\text{-}5b)$$

Input/Output Specifications. The data taken from the revised benchmark Problem 3.2 [Ward, et al., 1984b] are listed in Table 4.1-1. SWIFT II solves for pressure instead of drawdown, as specified in the benchmark problem. The transformation between the two is given by Equations (3.1-6) and (3.1-7). Benchmark Problem 3.2 requests the drawdown versus-time profile at a radius of 117.4 m from the with drawal well up to t = 10^6 s.

4.1.3 Numerical Simulation

Code Input. In the previous problem, conceptual one-dimensional local units have been placed within the global grid blocks to simulate dual-porosity effects. Furthermore, the units were assumed to only provide storage with a no-flow condition prescribed at one of its sides. In this problem, the role of these units is expanded and they are placed outside of the global aquifer block to simulate an aquitard. Figure 4.1.2 illustrates the numerical gridding including the global aquifer blocks and the one-dimensional aquitard units subdivided into grid blocks.

The code input for the local units is given in Figure 4.1-3. The control parameter

Table 4.1-1

Problem 5. Data

Parameter	Symbol	Value
Aquifer Transmissivity	T	0.05 m^2/s
Aquifer Hydraulic Conductivity	K	5.00 x 10^{-3} m/s
Aquifer Thickness	b	10 m
Porosity	Φ	0.10203
Water Density	ρ	1000 kg/m^3
Water Compressibility	c_w	0
Rock Compressibility	c_R	5.00 x 10^{-7} Pa^{-1}
Aquifer Storativity	S	0.005
Aquitard Specific Storativity	S_s'	0.0016 m^{-1}
Well Radius	r_w	0.1143 m
Aquitard Hydraulic Conductivity	K'	10^{-5} m/s
Aquitard Thickness	b'	50 m
Aquitard Porosity	Φ'	0.3265
Well Pumping Rate	Q	6.283 m^3/s

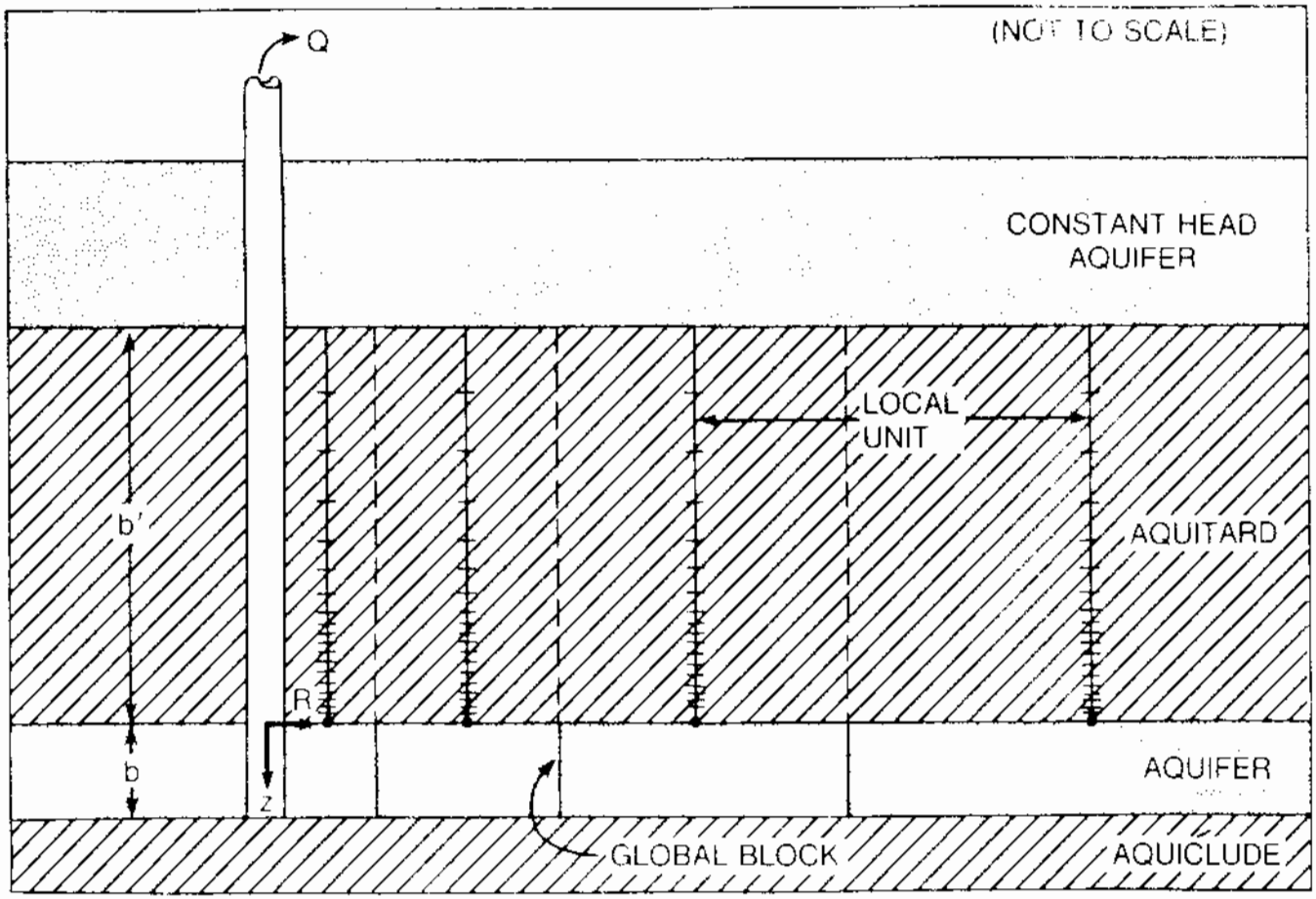

Figure 4.1-2. Model Grid of the Leaky-Aquifer System

```
PROBLEM NO. 5, SWIFT II EXAMPLE, SI UNITS, 03/86,                    M-1-1
FULLY PENETRATING WELL IN A LEAKY AQUIFER                            M-1-2
   1    0    0    0    1    0    0    1    0                        M-2
  50    1    1    3    0    1    1    2    0    1    0    1    0    0M-3-1
   0    1    1    1                                                 M-3-2
   0                                                                 ROD-1
  20                                                                 ROD-2
   1   30    1    1    1    1    1   -3                             ROD-3
                                                                     ROD-3-BLN
     0.0    5.0E-7       0.0       1.0       1.0                   R1-1
     1.0       1.0       1.0       1.0       1.0       1.0      1.0R1-2
  3000.0     5.0E5      20.0    1000.0    1000.0                    R1-3
     2    2    2    2                                               R1-6
    20.0     0.001      20.0     0.001                              R1-7
    0.20     0.001      0.80     0.001                              R1-8
   100.0     0.001     200.0     0.001                              R1-9
   100.0     0.001     200.0     0.001                              R1-10
     0.0      20.0                                                  R1-11
   100.0      20.0                                                  R1-11
   0    0                                                          R1-12
    20.0     5.0E5       0.0       0.0                            R1-16
  0.1143 0.1263842 2646.7663       0.0                            R1-22
    10.0    5.0E-3    5.0E-3 0.1020304       0.0                   R1-23
                                                                     R1-26 BLN
   3    0                                                          R1-27
   1    0    0                                                     R1-29
 5.0E-2 1.020304 2646.7663     360.0                               R1-31
                                                                     R1-33 BLN
 5.0E-7                                                           R1D-1
     0.0       0.0 0.3264973    1.0E-5       0.0       0.0      0.0R1D-2-1
   1    1      50.0      0.50       0.0                            R1D-2-2
   1    1    0    0    0                                         R1D-3-1
     0.0       0.0       0.0                                     R1D-3-2
                                                                     R1D-3 BLN
                                                                     R1D-5-BLN
   0    0    0                                                     I-1
     0.0                                                         R1A-1
   1    1    0    0    0    0    0    0    0    0                 R2-1
   4                                                             R2-4
   6.283       0.0       0.0                                     R2-5
   1    1    1    1    1    1                                    R2-7-1
   3.125       0.0      20.0       0.0                           R2-7-2
   2   35    1    1    1    1                                    R2-7-1
 1.0E10        0.0      20.0       0.0                           R2-7-2
   3   35    1    1    1    1                                    R2-7-1
 1.0E10        0.0      20.0       0.0                           R2-7-2
   4   35    1    1    1    1                                    R2-7-1
 1.0E10        0.0      20.0       0.0                           R2-7-2
                                                                     R2-7-BLN
     1.0       1.0
```

Figure 4.1.3. Problem 5. Listing of SWIFT II Input Data

```
1    1    1    1   -1    1  011    0 0000    0   00   -1  111   00R2-13
0    0    0    0    0    0    0    0    0    0                    R2-1
 1.0E3        0.0        0.0        0.0      1.0E4        0.0      1.0E3     0.05E3
1    1    1    1   -1    1  011    0 0000    0   00   -1  011   00R2-13
0    0    0    0    0    0    0    0    0    0                    R2-1
 1.0E4        0.0        0.0        0.0      1.0E4        0.0      1.0E4      0.1E4
1    1    1    1   -1    1  011    0 0000    0   00   -1  011   00R2-13
0    0    0    0    0    0    0    0    0    0                    R2-1
 1.0E5        0.0        0.0        0.0      1.0E4        0.0      1.0E5      0.1E5
1    1    1    1   -1    1  011    0 0000    0   00   -1  011   00R2-13
0    0    0    0    0    0    0    0    0    0                    R2-1
 1.0E6        0.0        0.0        0.0      1.0E4        0.0      1.0E6      0.2E6
1    1    1    1   -1    1  011    0 0000    0   00   -1  011   00R2-13
0    0    0    1    0    0    0    0    0    0                    R2-1-END
2      OBSERVATION WELL (R = 117.4 M)     SMALL TIME                P-2
   0.0       2.0E4      4.0E2      3.0E5      5.0E5        0 0       0.0P-3-1
   0.0         0.0        0.0        0.0                             P-3-2
0.40E3    4.835E5                                                    P-4
1.00E3    4.532E5                                                    P-4
2.00E3    4.230E5                                                    P-4
4.00E3    3.899E5                                                    P-4
10.0E3    3.447E5                                                    P-4
20.0E3    3.104E5                                                    P-4
 -100.                                                               P-4-END
3      OBSERVATION WELL (R = 117.4 M)   SMALL AND LARGE TIME        P-2
   0.0       4.0E5      8.0E3      1.6E5      3.2E5        0 0       0.0P-3-1
   0.0         0.0        0.0        0.0                             P-3-2
2.00E4    3.104E5                                                    P-4
4.00E4    2.763E5                                                    P-4
9.00E4    2.331E5                                                    P-4
10.0E4    2.314E5                                                    P-4
15.0E4    2.096E5                                                    P-4
20.0E4    1.975E5                                                    P-4
30.0E4    1.918E5                                                    P-4
40.0E4    1.637E5                                                    P-4
 -100.                                                               P-4-END
4      OBSERVATION WELL (R = 117.4 M)      LARGE TIME                P-2
   0.0       1.0E6      2.0E4      1.7E5      2.2E5        0.0       0.0P-3-1
   0.0         0.0        0.0        0.0                             P-3-2
1.50E5    2.096E5                                                    P-4
3.00E5    1.918E5                                                    P-4
5.00E5    1.873E5                                                    P-4
9.00E5    1.863E5                                                    P-4
 -100.                                                               P-4-END
                                                                     P-END
```

Figure 4.1-3. Problem 5. Listing of SWIFT II Input Data (Continued)

IFD = -3 , ROD-3 (4.1-6a)

sets local units outside all 50 grid blocks. The control parameter

KBC = 1 , R1D-3-1 (4.1-6b)

activates the external constant-pressure boundary condition, specified as

PBD = 0.0 , R1D-3-2 . (4.1-6c)

Figure 4.1-3 also provides the outer radius of the simulated region:

r_e = RE = 2647 m , R1-22

and was set to be larger than the radius of pressure response:

$$\tilde{r}_e = (Tb'/K')^{1/2} = 500 \text{ m} \quad . \qquad (4.1\text{-}7)$$

This quantity, derived from dimensional analysis, accounts for the effect of leakage from the neighboring aquifer on the extent of the drawdown cone.

Results. The numerical results are plotted in Figure 4.1-4 and include two asymptotic analytic solutions taken from Hantush [1960] for $t < (b')^2 S_s'/10K' = 4 \times 10^4$s and for $t > 2(b')^2 S_s'/K' = 8 \times 10^5$s. The agreement between the numerical and analytical results is good.

Code Output. This output (see microfiche listing) includes SWIFT II printer plots*. Because the code only plots data pertaining to wells, observation wells are

---

* The term "plot" should not be confused with the term "map." Maps refer to two-dimensional contours of pressure, isopleths, and isotherms. The mapping facility is not coupled to the presence of wells.

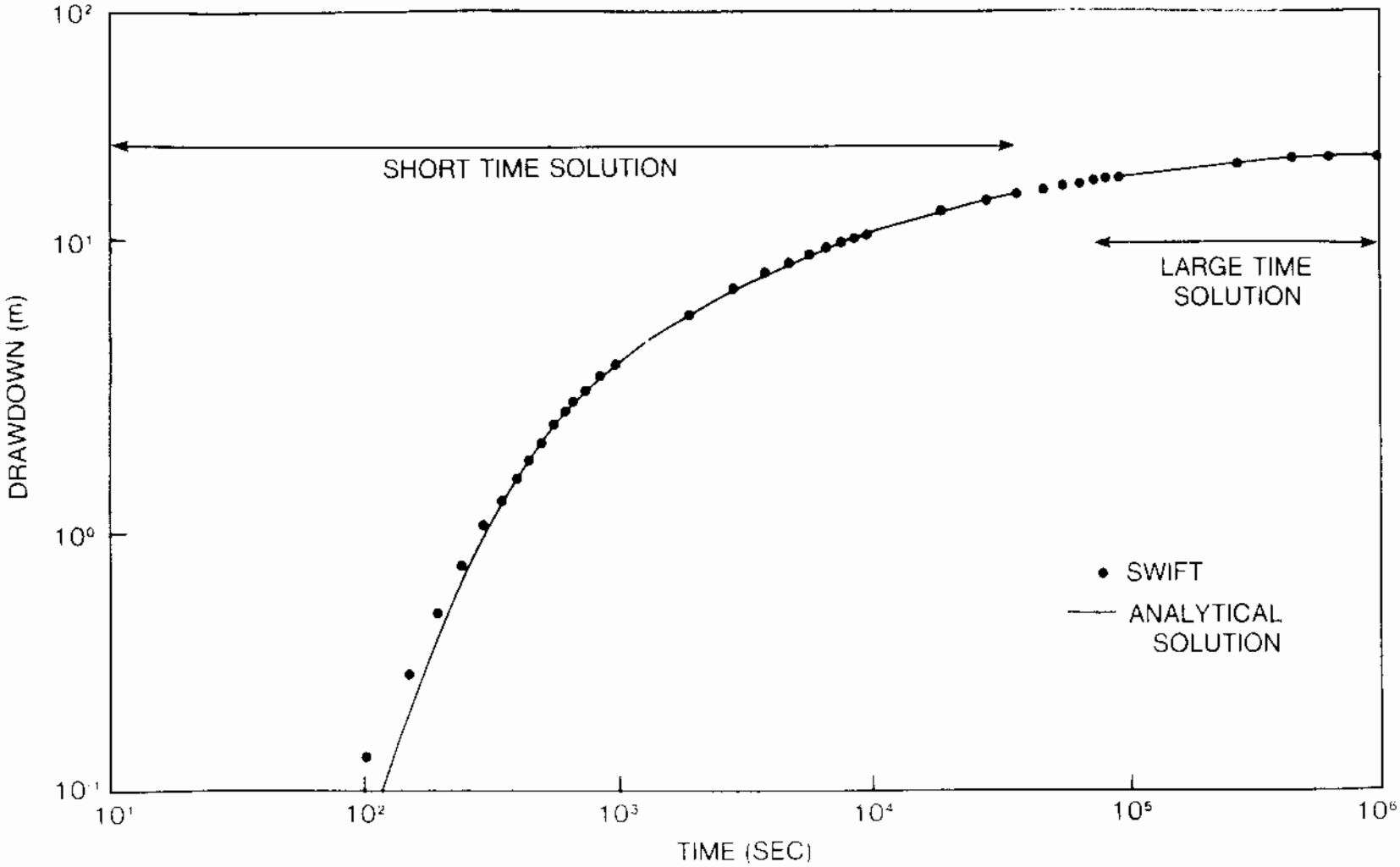

Figure 4.1-4. Results from SWIFT II and the Analytical Solutions of Hantush (1960) for a Radial Distance of 117.4 m

defined in Cards R2-4 through R2-7. Three wells are used to display drawdown at the time periods

$$0 \leq t \leq 2 \times 10^4 s, \quad 0 \leq t \leq 4 \times 10^5 s \text{ and } 0 \leq t \leq 10^6 s \qquad (4.1\text{-}8)$$

with different scales of resolution, permitting a detailed comparison with the Hantush [1960] analytic solutions.

Plotting is activated by a positive value of the plotting key NPLP = 1, (Card M-2), whose value appears in the initial table of the output listing (see microfiche).

4.2 PROBLEM 6. HEAT TRANSPORT DURING FLUID INJECTION [AVDONIN, 1964]

4.2.1 Objective

The objective of Problem 6 is to simulate convective heat transport resulting from injection of hot water into an aquifer with heat losses to the confining beds.

4.2.2 Problem Description

Problem Statement. An incompressible fluid with temperature, T_I, is injected into a confined aquifer with temperature, T_0, through a fully penetrating well (Figure 4.2-1). Both thermal convection and thermal conduction occur within the aquifer; while within the confining layers, denoted as over/underburden, only thermal conduction takes place.

Transport Equations. For the aquifer, the transport equation is

$$-v\rho c_p \frac{\partial T}{\partial r} + K_m \frac{1}{r} \frac{\partial}{\partial r} \left(r \frac{\partial T}{\partial r}\right) - \Gamma_H = \rho_m c_{pm} \frac{\partial T}{\partial t} \qquad (4.2\text{-}1)$$

and for the confining beds;

$$K'_m \frac{\partial^2 T'}{\partial z^2} + \Gamma_H = \rho'_m c'_m \frac{\partial T'}{\partial t} \quad . \qquad (4.2\text{-}2)$$

The coupling term is given by

$$\Gamma_H = -(2/b) K'_m \frac{\partial T}{\partial z} \quad . \qquad (4.2\text{-}3)$$

The fluid velocity is given by

$$v = Q/2\pi r b \rho \phi \quad . \qquad (4.2\text{-}4)$$

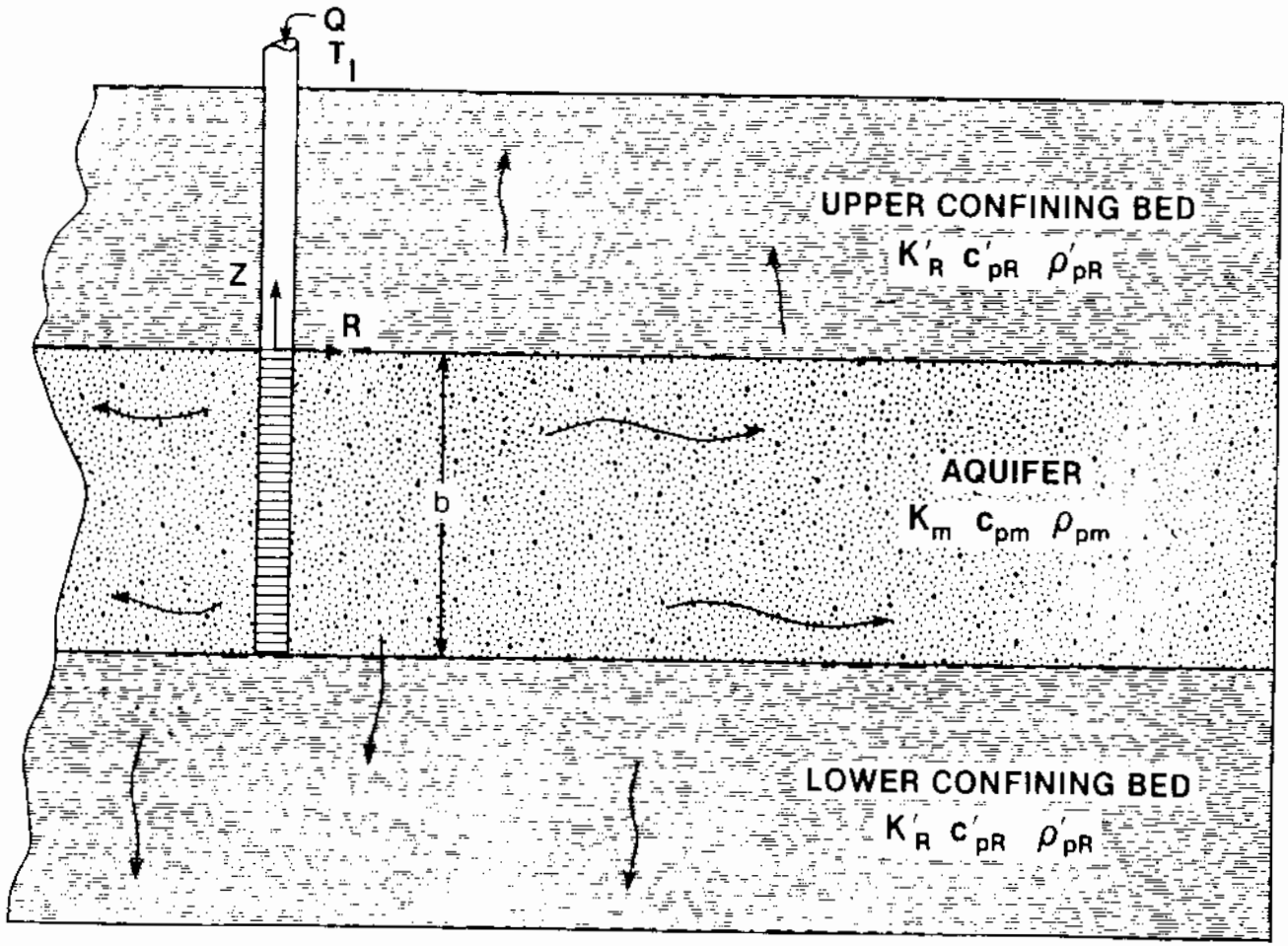

Figure 4.2-1. Problem 6. Radial Heat Transport Within an Aquifer with Losses to the Confining Beds

Initial/Boundary Conditions. The initial and boundary conditions for the aquifer are:

$$T(r,0) = T_o \qquad (4.2\text{-}5a)$$

$$T(0,t) = T_I \qquad (4.2\text{-}5b)$$

$$T(\infty,t) = T_o \qquad (4.2\text{-}5c)$$

and, for the overburden,

$$T'(r,z,0) = T_o \qquad (4.2\text{-}6a)$$

$$T'(r,\infty,t) = T_o \qquad (4.2\text{-}6b)$$

$$T'(r,0,t) = T(r) \qquad (4.2\text{-}6c)$$

and, for the underburden,

$$T'(r,z,0) = T_o \qquad (4.2\text{-}6d)$$

$$T'(r,-\infty,t) = T_o \qquad (4.2\text{-}6e)$$

$$T'(r,-b,t) = T(r) \qquad (4.2\text{-}6f)$$

where z is measured positive upward from the upper aquifer boundary.

Input/Output Specifications. The data was taken from the benchmarking Problem 5.1 [Ross, et al., 1982] and is presented in Table 4.2-1.

Using the composite values (subscript m) in the benchmark specifications, the values for the rock density and the rock heat capacities were chosen to be consistent with the relation:

$$\rho_m c_{pm} = \phi\ \rho c_p + (1-\phi)\rho_R c_{pR} \quad . \qquad (4.2\text{-}7)$$

The output specified in benchmark Problem 5.1 [Ross et al., 1982] calls for the thermal breakthrough at a radius of 37.5 m from the injection well up to $t = 10^9$ s.

Table 4.2-1

Problem 6. Data

Parameter	Symbol	Value
Injection Rate	Q	10 kg/s
Injection Temperature	T_1	160°C
Initial Temperature	T_0	170°C
Over/Underburden		
Thermal Conductivity	K'_m	20 W/(m °C)
Density	ρ'_m	2500 kg/m^3
Heat Capacity, Composite	c'_{pm}	1000 J/(kg °C)
Porosity	Φ'	0.2
Aquifer		
Thermal Conductivity	K_m	20 W/(m °C)
Density	ρ_m	2500 kg/m^3
Heat Capacity, Composite	c_{pm}	1000 J/(kg °C)
Thickness	b	100 m
Porosity	Φ	0.2
Heat Capacity, Water	c_p	4185 J/(kg °C)
Heat Capacity, Rock	c_{pR}	2.079 x 10^6 J/(M^3 °C)
Well Radius	r_w	0.766 m

4.2.3 Numerical Simulation

Code Input. For computer efficiency, it is desirable to minimize the extent of the simulated system and, at the same time, adequately describe the infinite domain. It is also desirable to use the coarsest mesh possible in space and time and still adequately simulate the thermal behavior at a radius r = 37.5 m from the injection well. Within the aquifer, the controlling mechanism is flow, which dominates the convective heat transport. For steady flow, Equation 4.2-4 gives the fluid velocity which is insured by imposing a constant pressure condition at the external radius (Card R1-28.2 of Figure 4.2-2).

The external radius must be sufficiently large to contain the movement of the thermal front. This radius is calculated as follows:

$$\bar{v} = v\rho c_p/\rho_m c_{pm} = \bar{v}_o/r \qquad (4.2\text{-}8a)$$

and using Equation (4.2-4) and the values in Table 4.2 1,

$$\bar{v}_o = Qc_p/2\pi b\phi\rho_m c_{pm} = 1.332 \times 10^{-4}\ m^2/s \quad . \qquad (4.2\text{-}8b)$$

The distance traveled by the thermal front in $t = 10^9$ s is then

$$\tilde{r} = (\bar{v}_o t)^{1/2} = 370\ m \quad . \qquad (4.2\ 9a)$$

To account for possible conductive dispersion of the front and include a minimum safety factor, the external radius is chosen to be

$$r_e = 1000\ m \quad , \quad R1\text{-}22 \quad . \qquad (4.2\text{-}9b)$$

Gridding criteria are unknown in this case, and consequently, a trial and-error procedure was used to determine the spatial and temporal domains. Thermal conduction dominates within the over/underburden. The extent of the thermal front at $t = 10^9$ s is

```
PROBLEM NO. 6, SWIFT II EXAMPLE, SI UNITS, 03/86,                       M-1-1
AVDONIN RADIAL HEAT TRANSPORT WITH LOSS TO CONFINING BEDS               M-1-2
   -2     0     0     0     0     1     0     1     0                   M-2
   30     1     1     3     0     1     1     0     0     1     0     0     0    0M-3-1
    0     1     1     1                                                 M-3-2
    0                                                                   ROD-1
   15                                                                   ROD-2
    1    30     1     1     1     1     1     3                         ROD-3
                                                                        ROD-3-BLN
 3.20E-15          0.0           0.0        4185.0 2.07875E6           R1-1
     20.0          20.0          20.0          1.0          0.0    0.0 1.00E-50R1-2
   287.3  5.00E 06          160.0         1000.0        1000.0          R1-3
    0     1     1     2                                                 R1-6
    160.0         0.001         160.0         0.001                     R1-7
    170.0         0.001                                                 R1-9
    170.0         0.001                                                 R1-10
      0.0         170.0                                                 R1-11
   100000.0       170.0                                                 R1-11
    0     0                                                             R1-12
     170.          0.0           0.0           0.0                     R1-16
 .090223       .7655922        1000.           0.0                     R1-22
    100.0         9.8E-6        9.8E-6          0.20                    R1-23
                                                                        R1-26 BLN
    4     0                                                             R1-27
   30    30     1     1     1     1     0                               R1-28-1
      2.0           0.0         170.0           0.0           0.0       R1-28-2
                                                                        R1-28-BLN
                                                                        R1-33-BLN
      0.0                                                               R1D-1
      0.0           0.0           0.20        9.8E-6          0.0    20.0 2.0/8/5E6R1D-2-1
    1     1         300.0          10.0           0.0                   R1D-2-2
                                                                        R1D-3-BLN
                                                                        R1D-5-BLN
    0     0     0                                                       1-3
      0.0                                                               R1A-2
    1     1     1     0     0     0     0     0     0                   R2-1
    1         0.5                                                       R2-2
    2                                                                   R2-4
   -0.010         0.0                                                 R2-5
    1     1     1     1     1     1                                     R2-7-1
      1.0           0.0         160.0           0.0                   R2-7-2
    2    17     1     1     1     1                                     R2-7-1
      1.0           0.0           0.0           0.0                   R2-7-2
                                                                        R2-7-BLN
   1.00E4        1.00E4                                                
    1     1     1     1     1     1   000     0 0000     0    00    -1  001   00R2-13
    0     0     0     0     0     0     0     0     0                   R2-1
   1.00E5          0.0           0.0           0.0           0.0       1.0    0.50E5    0.10E5
    1     1     1     1     1     1   000     0 0000     0    00    -1  111   00R2-13
    0     0     0     0     0     0     0     0     0                   R2-1
```

Figure 4.2-2. Problem 6. Listing of SWIFT II Input Data

```
   1.00E6        0.0        0.0        0.0        0.0        1.0    0.50E6     0.10E6
   1    1    1    1    1    1  000    0 0000    0   00   -1  101    00R2-13
   0    0    0    0    0    0    0    0    0                        R2-1
   1.00E7        0.0        0.0        0.0        0.0        1.0    0.50E7     0.10E7
   1    1    1    1    1    1  000    0 0000    0   00   -1  111    00R2-13
   0    0    0    0    0    0    0    0    0                        R2-1
   1.00E8        0.0        0.0        0.0        0.0        1.0    0.50E8     0.10E8
   1    1    1    1    1    1  000    0 0000    0   00   -1  101    13R2-13
   0    0    0    0    0    0    0    0    0                        R2-1
   1.00E9        0.0        0.0        0.0        0.0        1.0    0.50E9     0.20E8
   1    1    1    1    1    1  000    0 0000    0   00   -1  101    00R2-13
   0    0    0    1    0    0    0    0    0                        R2-1-END
   1      OBSERVATION WELL (R=3.7 : METE                            P-2
      0.0  1.00E 09  2.00E 07        0.0        0 0        0 0        0.0P-3-1
    160.0     170.0        0.0        0 0                           P-3-2
 1.10E 07                          169.70                           P-4
 1.59E 07                          169.03                           P-4
 2.34E 07                          167.81                           P-4
3.409E 07                          166.35                           P-4
5.051E 07                          164.87                           P-4
 7.48E 07                          163.64                           P-4
 9.26E 07                          163.09                           P-4
1.138E 08                          162.65                           P-4
1.403E 08                          162.27                           P-4
 1.75E 08                          161.94                           P-4
2.197E 08                          161.65                           P-4
2.579E 08                          161.42                           P-4
 3.50E 08                          161.22                           P-4
 4.50E 08                          161.05                           P-4
 5.50E 08                          160.93                           P-4
 6.50E 08                          160.84                           P-4
 7.50E 08                          160.78                           P-4
 8.50E 08                          160.73                           P-4
 9.50E 08                          160.68                           P-4
 1.00E 09                          160.66                           P-4
   -100.0                                                           P-4-END
   0                                                                P STOP
```

Figure 4.2-2. Problem 6. Listing of SWIFT II Input Data (Continued)

$$\tilde{a} = (K'_m t/\rho'_m c'_{pm})^{1/2} = 90 \text{ m} \quad . \qquad (4.2\text{-}10a)$$

However,

$$a = 300 \text{ m} \quad , \quad \text{RID-2-2} \qquad (4.2\text{-}10b)$$

is assigned as the simulated thickness of the confining beds. A fine mesh has been chosen to increase resolution in the over/underburden.

Results. The numerical results and the analytical solution of Avdonin [1964] are displayed in Figure 4.2-3. When only heat transport within the aquifer is considered, the effect of conduction within the over/underburden is relatively small. The small difference between the numerical and analytical solutions could be attributed to some numerical dispersion, arising from convection in the aquifer.

Code Output. The microfiche provides a listing of the code output. It includes: (1) an echo of the input data, (2) the radial gridding within the aquifer and the linear grid within the confining beds, (3) time-step and well summaries, (4) a steady-state pressure distribution and (5) time-dependent temperature distributions within the aquifer and the confining beds.

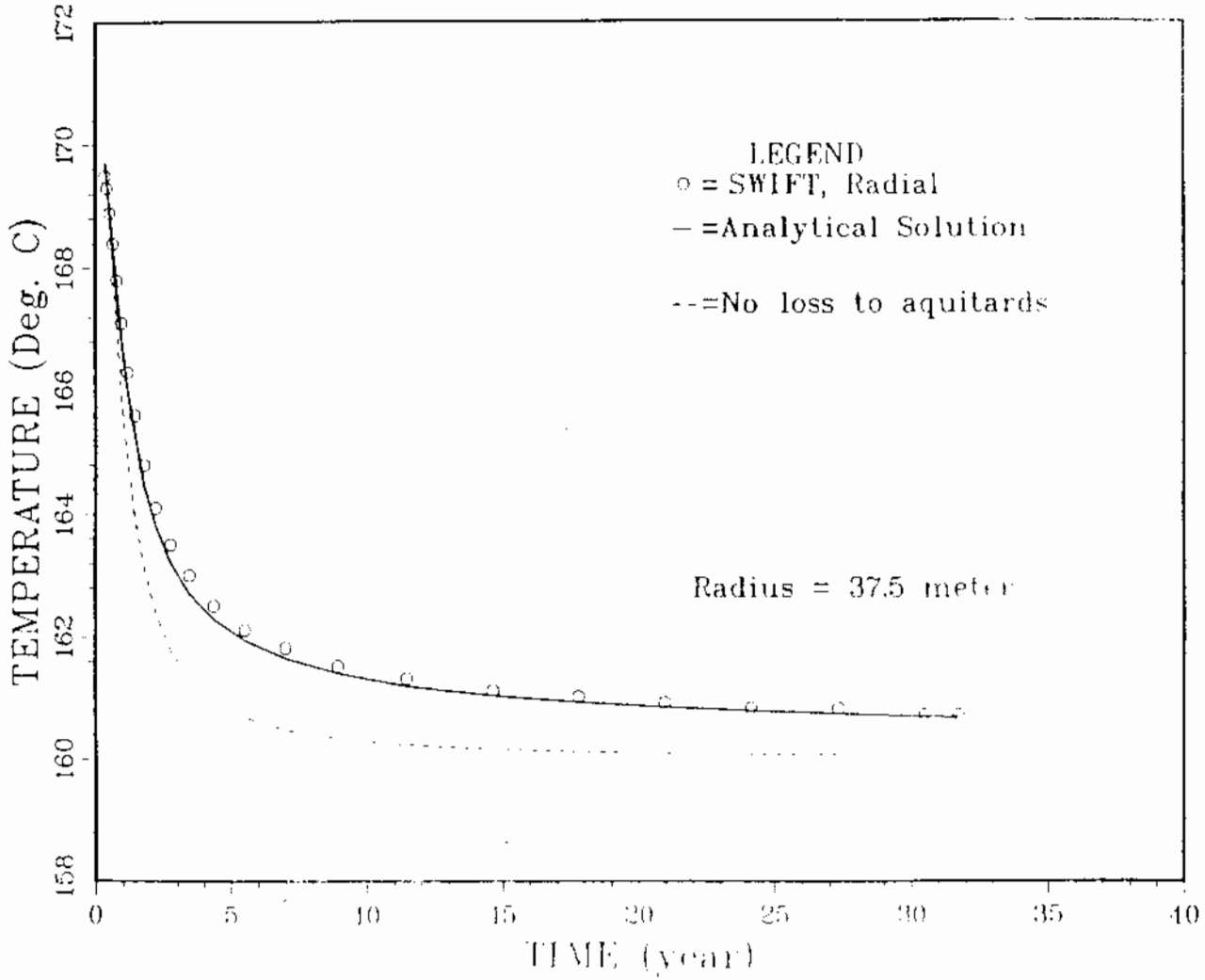

Figure 4.2-3. Temperature Breakthrough Within the Aquifer at 37.5 m from the Injection Well

5. FLOW WITH A FREE WATER SURFACE

5.1 PROBLEM 7. THE DUPUIT-FORCHHEIMER STEADY-STATE PROBLEM (BEAR, 1972)

5.1.1 Objective

The objective of Problem 7 is to simulate steady-state flow in a phreatic aquifer.

5.1.2 Description of the Problem

Problem Statement. In Problem 7, a phreatic aquifer of length L (Figure 5.1-1) with fixed free-water elevations

$$h(0) = h_0 \tag{5.1-1a}$$

and

$$h(L) = h_L \tag{5.1-1b}$$

is subjected to surface recharge at a rate q. The objective is to determine the elevation h(x) of the free water surface. Hydraulic properties are given in Table 5.1-1.

Analytical Solution. The analytical solution (Bear, 1972) neglects vertical flow:

$$u_z = -K_z \partial H/\partial z = 0 \tag{5.1-2a}$$

and yields a one-dimensional solution in the x coordinate. Here H is the total head, H = h - z. The transmissivity is a function of the saturated thickness:

$$T = K_x h \quad . \tag{5.1-2b}$$

and the total discharge through a vertical surface unit width in the y direction (Figure 5.1-1), is given by

$$u_x = -T \frac{\partial h}{\partial x} \quad . \tag{5.1-3}$$

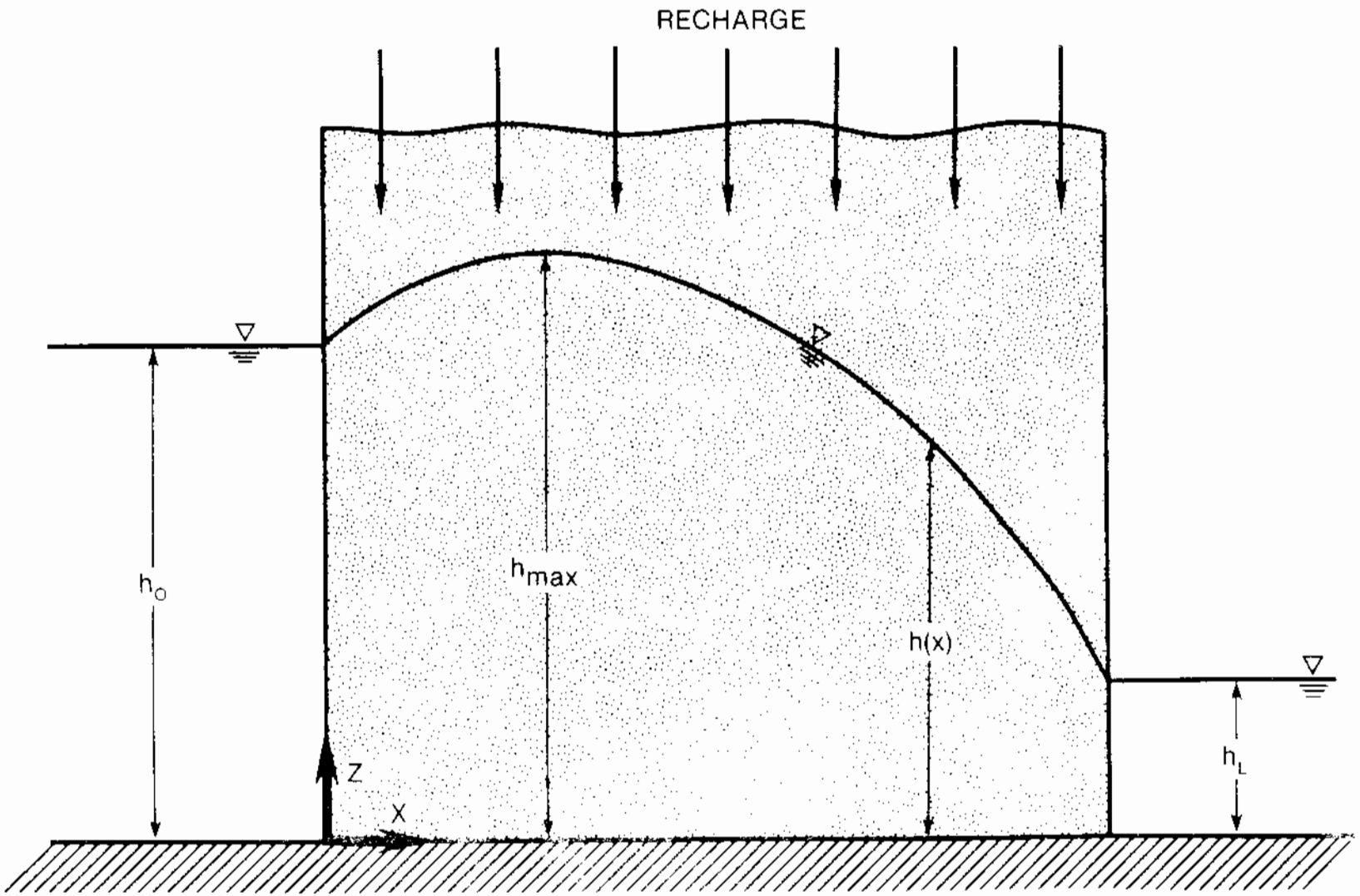

Figure 5.1-1. Problem 7. Diagram for the Dupuit-Forchheimer Problem

Table 5.1-1

Problem 7. Data

Parameter	Symbol	Value
Surface Recharge	q	7.505×10^{-5} m/s
Lateral Conductivity	K_x	0.03 m/s
Vertical Conductivity	K_z	0.03 m/s
Height of Free-Water Surface at x = 0	h_o	0.75 m
Height of Free-Water Surface at x = L	h_L	0.25 m
Length of System	L	20 m

The equation of continuity at steady state is [Bear, 1972]

$$\frac{\partial}{\partial x}\left(K_x h \frac{\partial h}{\partial x}\right) + q = 0 \quad , \tag{5.1-4}$$

which is the Forchheimer equation. The analytical solution of Equation (5.1-4) is the Dupuit-Forchheimer parabola:

$$h^2 - h_o^2 = (h_L^2 - h_o^2)x/L + (q/K_x)(L-x)x \quad . \tag{5.1-5}$$

The flow rates at the boundaries are given by

$$\begin{matrix} u_o \\ u_L \end{matrix} = (K_x/2L)(h_o^2 - h_L^2) + \begin{pmatrix} (-) \\ (+) \end{pmatrix} (qL/2) \quad . \tag{5.1-6}$$

The first term on the right-hand side represents the flow due to the difference in heads across the system. This rate is the same for both ends. The second term arises from the surface recharge.

5.1.3 Numerical Solution.

The numerical solution with SWIFT II uses a two-dimensional vertical cross section gridded as specified in Cards R2-17 through R2-19 (Figure 5.1-2). The following hydrostatic conditions

$$\tilde{p} = p - \rho(g/g_c)h = \text{constant} \tag{5.1-7}$$

are prescribed at the side boundaries (Cards R1-27 and R1-28). The effects of the vertical flow in the two-dimensional grid were negligible for this problem.

The full thickness, Δz, is used in calculating the transmissivity of a saturated grid block. For a partially saturated grid block, only the saturated thickness Δh is used:

$$T_x = K_x \Delta h \quad . \tag{5.1-8}$$

```
PROBLEM NO. 7, SWIFT II EXAMPLE, SI UNITS, 03/86,                          M-1.1
DUPUIT-FORCHHEIMER STEADY-STATE FREEWATER SURFACE WITH RECHARGE             M-1.2
   4    0    0    1    0    0    0    1    0                               M-2
  20    1   20    1    0    1    0    2    0   20   20    0    0  0M-3-1
   0    0    0    0                                                        M-3.2
     0.0       0.0       0.0       1.0       1.0                          R1-1
     0.0       0.0       0.0       0.0       1.0       1.0  1.0E-10R1-2
  2130.0   3.00E07      20.0    1000.0    1000.0                          R1-3
   0    2    2    2                                                        R1-6
    20.0  1.00E-03      20.0  1.00E-03                                     R1-7
    40.0  1.00E-03      80.0  1.00E-03                                     R1-9
    40.0  1.00E-03      80.0  1.00E-03                                     R1-10
     0.0      20.0                                                        R1-11
   600.0      20.0                                                        R1-13
   0    0                                                                 R1-12
    20.0       0.0       0.0       0.0                                   R1-16
  20*1.0
     1.0
  20*0.050
     0.03      0.03      0.03      0.50      0.0       0.0       0.0 0R1-30
                                                                          R1-26-R1-2
   4    1                                                                R1-
   1    1    1    1    6    6                                           R1-
        1.     244.2                                                     R1-
   1    1    1    1    7    7                                           R1-
        1.     732.6                                                     R1-
   1    1    1    1    8    8                                           R1-
        1.    1221.0                                                     R1-
   1    1    1    1    9    9                                           R1-
        1.    1709.4                                                     R1-
   1    1    1    1   10   10                                           R1-
        1.    2197.8                                                     R1-
   1    1    1    1   11   11                                           R1-
        1.    2686.2                                                     R1-
   1    1    1    1   12   12                                           R1-
        1.    3174.6                                                     R1-
   1    1    1    1   13   13                                           R1-
        1.    3663.0                                                     R1-
   1    1    1    1   14   14                                           R1-
        1.    4151.4                                                     R1-
   1    1    1    1   15   15                                           R1-
        1     4639.8                                                     R1-
   1    1    1    1   16   16                                           R1-
        1.    5128.2                                                     R1-
   1    1    1    1   17   17                                           R1-
        1.    5616.6                                                     R1-
   1    1    1    1   18   18                                           R1-
        1.    6105.0                                                     R1-
   1    1    1    1   19   19                                           R1-
        1.    6593.4                                                     R1-
   1    1    1    1   20   20                                           R1-
        1.    7081.8                                                     R1-
  20   20    1    1   16   16                                           R1-
        2.     244.2                                                     R1-
```

Figure 5.1-2. Problem 7. Listing of SWIFT II Input Data

```
20    20      1     1    17    17                                                  R1-28
      2.     732.6                                                                R1-28
20    20      1     1    18    18                                                  R1-28
      2.    1221.0                                                                R1-28
20    20      1     1    19    19                                                  R1-28
      2.    1709.4                                                                R1-28
20    20      1     1    20    20                                                  R1-28
      2.    2197.8                                                                R1-28
                                                                                  R1-28-BLS
                                                                                  R1-33-BLS
 0     0      0                                                                   I-1
    0.0                                                                           R1A-2
 3     3      0     0     0     2     0     1     0     1                        R2-1
 1    20      1     1 7.505E 05                                                   R2-2.5
                                                                                  R2-2.5-BLS
 3    20      0                                                                   R2-11
    0.0          0.0
 1     1      1     1     1     1   011     0 0000     0     1                    R2-13
 0     0      0     1     0     0     0     0     0                              R2-1 STOP
```

Figure 5.1-2. Problem 7. Listing of SWIFT II Input Data (Continued)

Results. The results of the numerical and analytical solutions are plotted in Figure 5.1-3. The same numerical solution is plotted relative to the grid blocks in Figure 5.1-4. The flows are

$$u_L \text{ (SWIFT)} = 1.1045 \times 10^{-3} \text{ m}^3/\text{s/m} \qquad (5.1\text{-}9a)$$

and

$$u_L \text{ (analytic)} = 1.1255 \times 10^{-3} \text{ m}^3/\text{s/m} \qquad (5.1\text{-}9a)$$

a difference of about 2 percent

Discussion of the Code Output. Water table elevations are obtained from the table of grid-block saturations, and the flow rate, u_L, is taken from the table of aquifer influx rates (see microfiche). The printing of the former table is controlled by IIPRT, and the latter by I06, both are specified on Card R2-13. Interpretation of these tables requires some additional data from the output. For example, examining the water-table elevation, it is noticed that the maximum water table elevation occurs within block I = 6, K = 5. The saturation in this grid block is

$$\bar{S}\ (6,5) = 0.8968 \qquad (5.1\text{-}10a)$$

Grid-block tables, located near the beginning of the output, are used to convert the grid-block saturation to the elevation

$$h\ (6,5) = 0.795 \text{ m} \quad . \qquad (5.1\text{-}10b)$$

The table for the aquifer-influence block numbers is needed to interpret the aquifer-influx rates. For the boundary x = 0, the aquifer-influx blocks are "1" through "15," and for the boundary x = L, the blocks are labelled "16" through "20". To obtain the flow in Equation (5.1-9), the sum of flow over grid blocks 16 through 20 is calculated,

$$u_L = \sum_{N=16}^{20} u_{LN} = 1.1045 \text{ kg/s/m} = 1.1045 \times 10^{-3} \text{ m}^3/\text{s/m} \quad . \qquad (5.1\text{-}11)$$

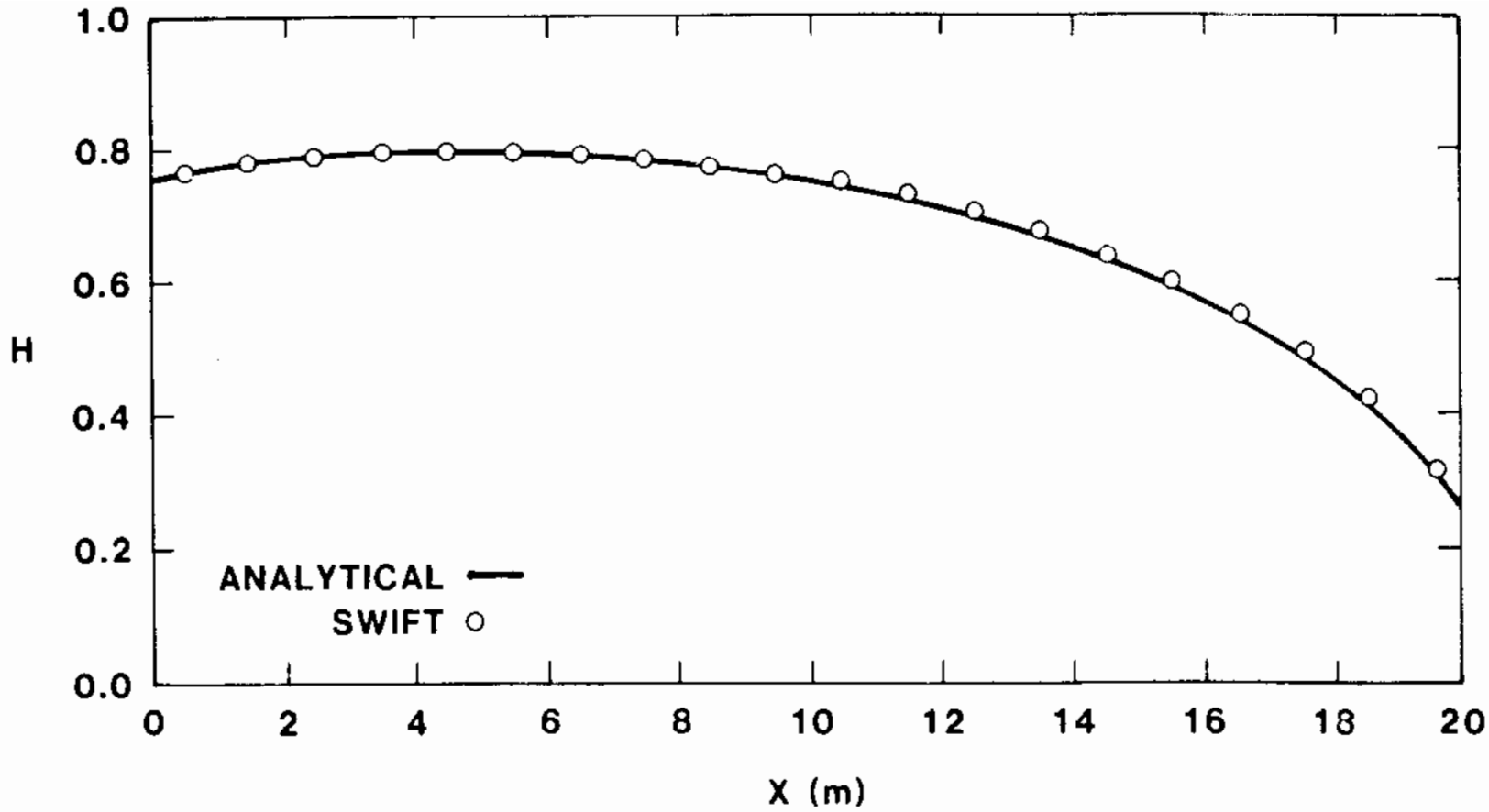

Figure 5.1-3. Steady-State Free-Water Surface for the Dupuit-Forchheimer Problem

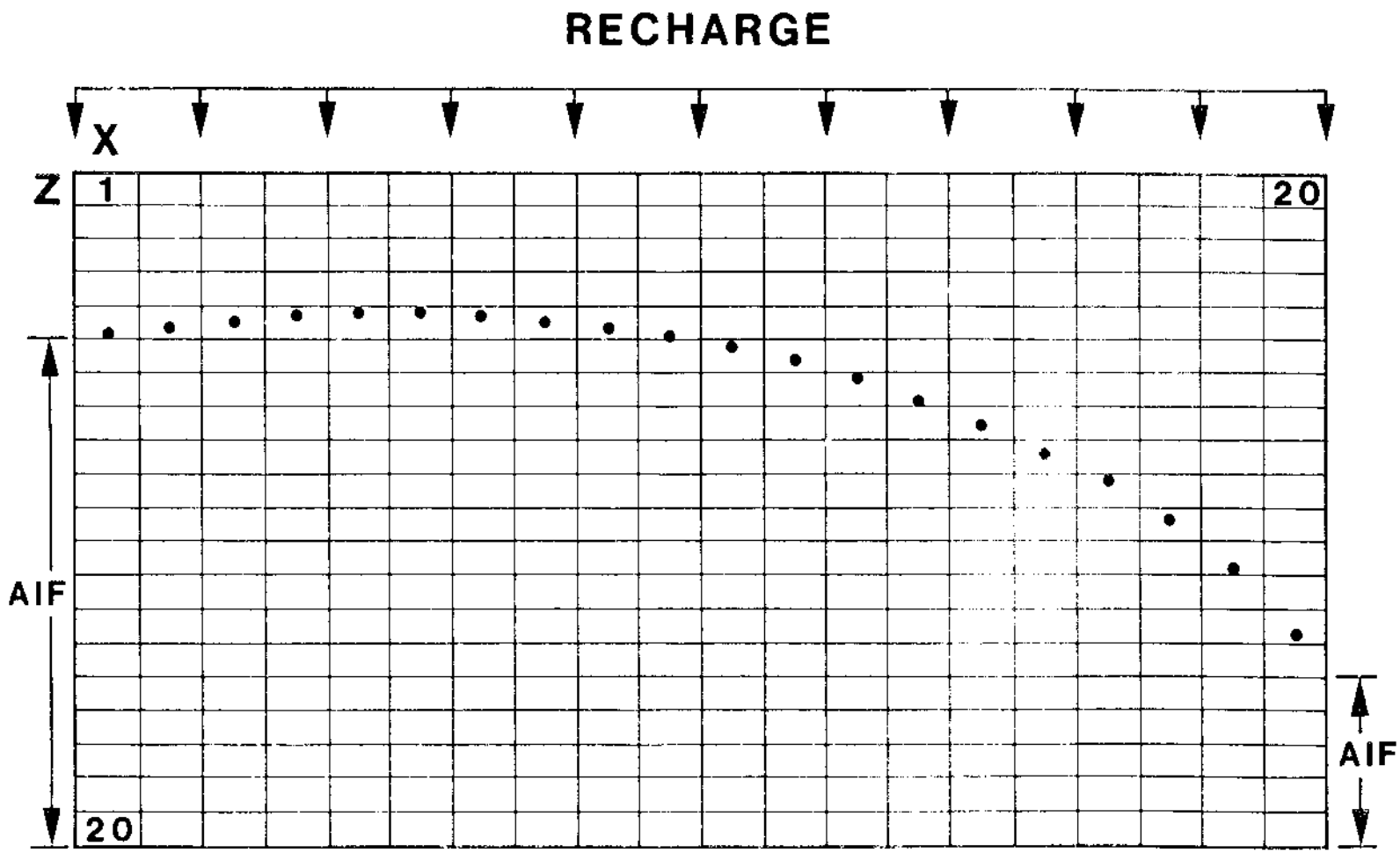

Figure 5.1-4. Gridding, Boundary Conditions (Labelled "AIF") and Recharge

5.2 PROBLEM 8. THE BOUSSINESQ TRANSIENT STATE PROBLEM [BEAR, 1972]

5.2.1 Objective

The objective of Problem 8 is to simulate time-dependent flow in a phreatic aquifer.

5.2.2 Problem Description

Problem Statement. The problem considered is a semi-infinite phreatic aquifer (Figure 5.2-1), completely saturated initially so that

$$h(x,0) = h_o \quad . \tag{5.2-1a}$$

For $t > 0$, the saturated thickness at one end is reduced to half its original amount,

$$h(0,t) = h_o/2 \tag{5.2-1b}$$

with no recharge through the upper surface. The objective is to determine the elevation of the free-water surface $h(x,t)$ as a function of position and time using the parameters given in Table 5.2-1.

Analytical Solution. The transmissivity is taken to be proportional to the saturated thickness h and flow is assumed to be horizontal. The equation of continuity [Bear, 1972] is

$$\frac{\partial}{\partial x}\left(K_x h \frac{\partial h}{\partial x}\right) = \Phi \frac{\partial h}{\partial t} \tag{5.2-2}$$

which is the Boussinesq equation. The Polubarinova Kochina [Bear, 1972, p. 384] general solution for this nonlinear equation is presented in Figure 5.2-2.

5.2.3 Numerical Solution

Code Input. A two-dimensional grid (Figure 5.2-3 and Card M-3-1) is used for the numerical simulation as opposed to the one dimensional analytical simulation. Horizontal flow is then approximated by choosing a relatively large vertical conductivity K_z (Card R1-20). As in the previous problem, the transmissivity is assumed to be proportional to the saturated thickness. A similar treatment is used for the storage coefficient. That is, the grid-block saturation

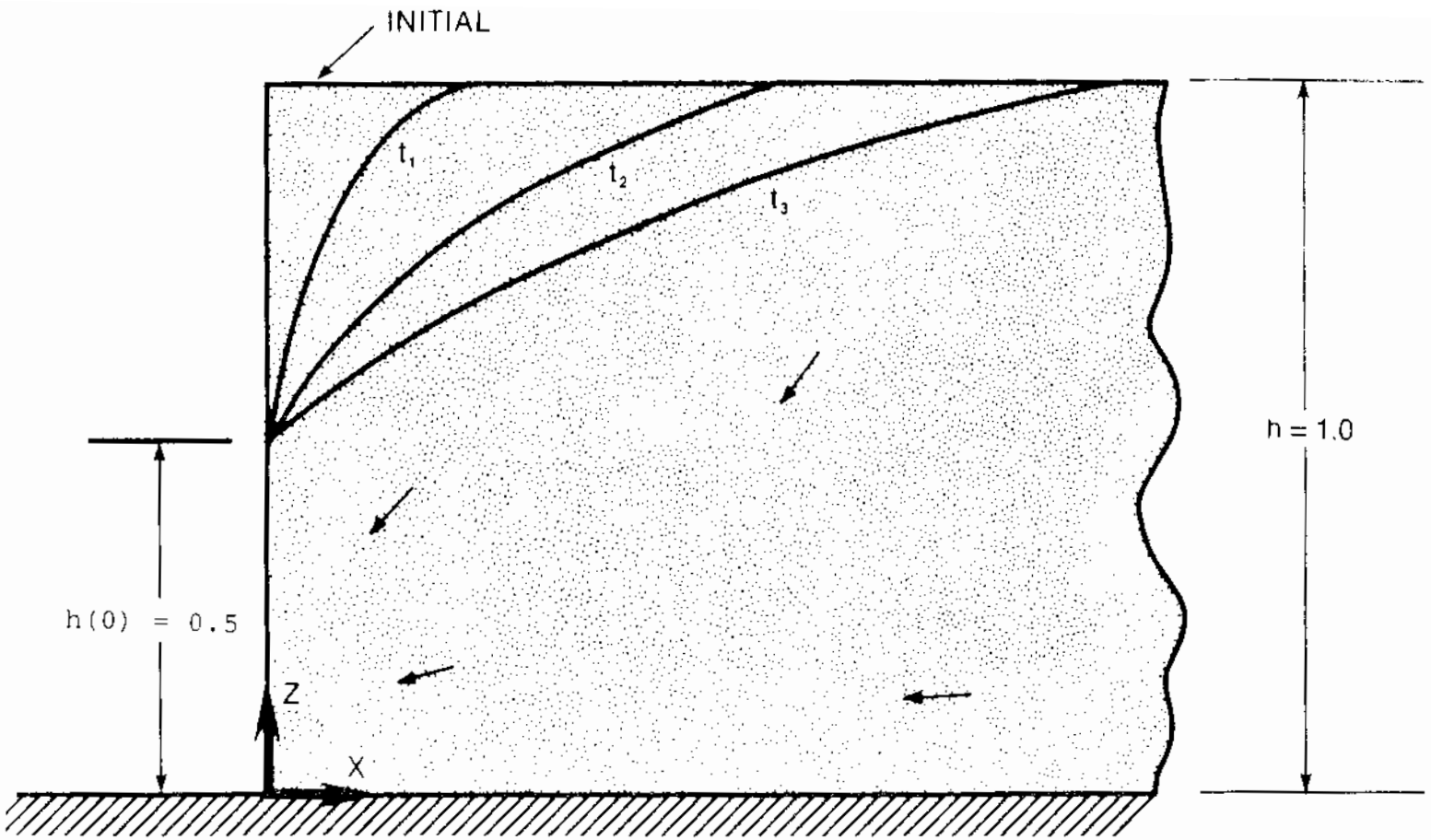

Figure 5.2-1. Problem 8. Diagram of the Boussinesq Problem

Table 5.2-1

Problem 8. Data

Parameter	Symbol	Value
Lateral Conductivity	K_x	0.01 m/s
Vertical Conductivity*	K_z	100.0 m/s
Porosity	ϕ	0.50
Initial Height of Free-Water Surface	h_o	1.0 m
Height of Free-Water Surface at x = 0	$h_o/2$	0.50 m

* Adjusted to a suitably large value to produce only horizontal flow.

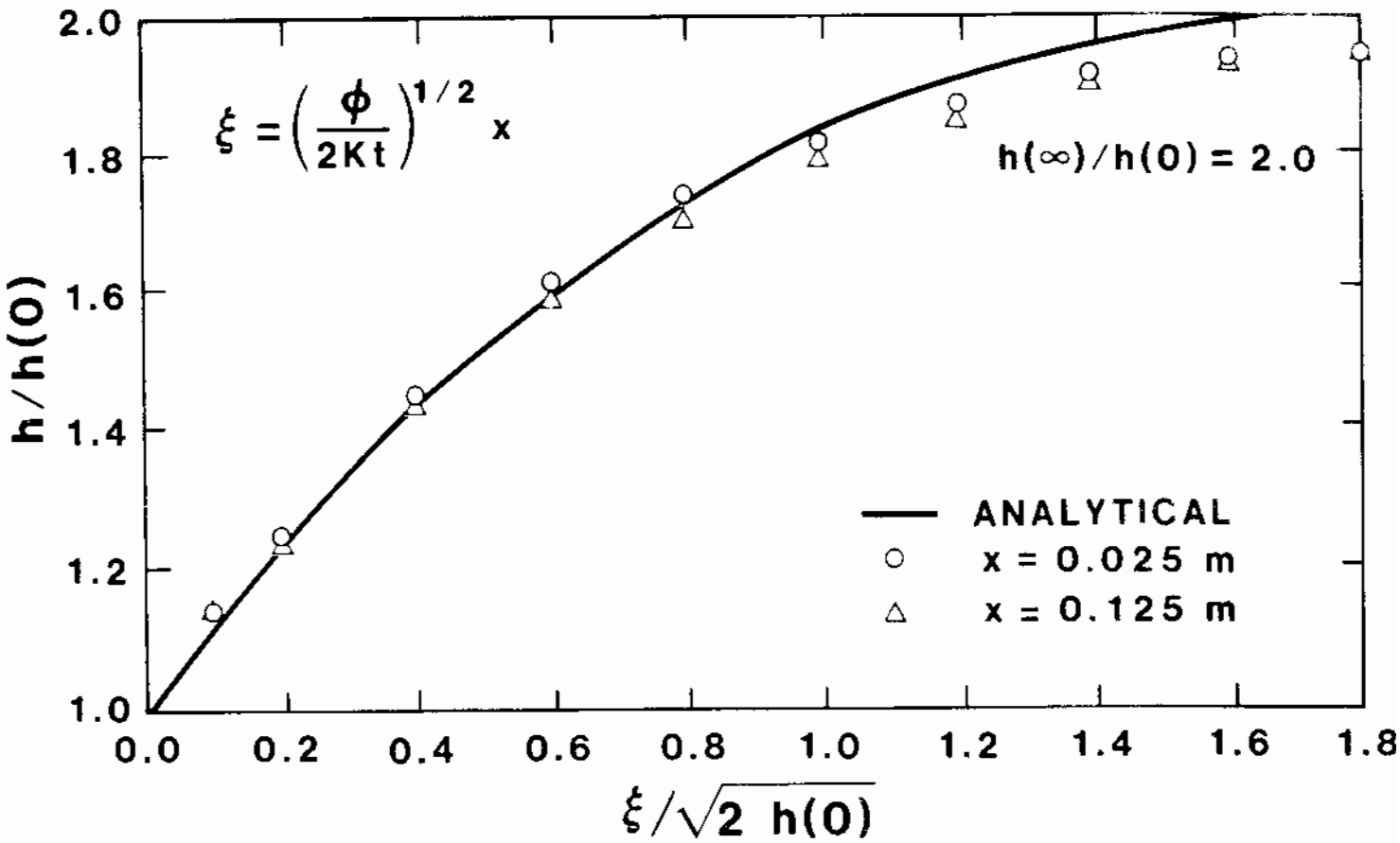

Figure 5.2-2. Time-dependent Free-Water Surface Elevation for the Boussinesq Problem

```
PROBLEM NO. 8, SWIFT II EXAMPLE, SI UNITS, 03/86,                       M-1-1
BOUSSINESQ'S EQN. - TRANSIENT FREE-WATER DESATURATION FROM INIT. SAT. M-1-2
    1     0     0     1     0     0     0     1     0                   M-2
   20     1    20     1     0     1     0     2     0    10     0     0     0    0M-3-1
    0     0     0                                                       M-3-2
 1.00E-10          0.0         0.0         1.0         1.0                R1-1
      0.0          0.0         0.0         0.0         1.0       1.0  1.00E-10R1-2
   2130.0    1.00E 07         20.0      1000.0      1000.0                R1-3
    0     2     2     2                                                 R1-6
     20.0    1.00E-03         20.0    1.00E-03                          R1-7
     40.0    1.00E-03         80.0    1.00E-03                          R1-9
     40.0    1.00E-03         80.0    1.00E-03                          R1-10
      0.0        20.0                                                   R1-11
   1000.0        20.0                                                   R1-13
    0     0                                                             R1-12
     20.0         0.0        -.025       -.025                         R1-16
   5*0.01      5*0.05      5*0.10      2*0.50      2*1.0       2.0
      1.0
  20*0.050
     0.01         1.0       100.0         0.50        0.0       0.0       0.0R1-20
                                                                         R1-20-NEW
    4     1                                                             R1-22
    1     1     1     1    11    11                                     R1-28-1
       1.       244.2                                                  R1-28-2
    1     1     1     1    12    12                                     R1-28-1
       1.       732.6                                                  R1-28-2
    1     1     1     1    13    13                                     R1-28-1
       1.      1221.1                                                  R1-28-2
    1     1     1     1    14    14                                     R1-28-1
       1.      1709.5                                                  R1-28-2
    1     1     1     1    15    15                                     R1-28-1
       1.      2197.9                                                  R1-28-2
    1     1     1     1    16    16                                     R1-28-1
       1.      2686.3                                                  R1-28-2
    1     1     1     1    17    17                                     R1-28-1
       1.      3174.7                                                  R1-28-2
    1     1     1     1    18    18                                     R1-28-1
       1.      3663.2                                                  R1-28-2
    1     1     1     1    19    19                                     R1-28-1
       1.      4151.6                                                  R1-28-2
    1     1     1     1    20    20                                     R1-28-1
       1.      4640.0                                                  R1-28-2
                                                                         R1-28-BCN
                                                                         R1-32-BCN
    0     0     0                                                       1-1
      0.0                                                              R1A-2
    0     0     0     0     0     0     0     0     0     0             R2-1
```

Figure 5.2-3. Problem 8. Listing of SWIFT II Input Data

```
 1.00E-07  1.00E-07
   0     1     0     1     1     0   111     0 0000     0     0                 R2-13
   0     0     0     0     0     0     0     0    0     0     0                 R2-1
 6.25E-04 6.249E-04
   1     1     1     1     1     1   111     0 0000     0    11                 R2-13
   0     0     0     0     0     0     0     0    0     0                       R2-1
9.76563E-43.51563E-4
   1     1     1     1     1     1   111     0 0000     0     0                 R2-13
   0     0     0     0     0     0     0     0    0     0                       R2-1
1.76311E-37.8654?E-4
   1     1     1     1     1     1   111     0 0000     0     0                 R2-13
   0     0     0     0     0     0     0     0    0     0                       R2-1
[illegible]        0.0         0.0         0.0     1000.0          0.0       6.0  6.25E-04
   1     1     1     1     1     1   111     0 0000     0     0                 R2-13
   0     0     0     0     0     0     0     0    0     0                       R2-1
1.5625E-02         0.0         0.0         0.0     1000.0          0.0       6.0  6.25E-04
   1     1     0     1     1     1   111     0 0000     0    11                 R2-13
   0     0     0     0     0     0     0     0    0     0                       R2-1
 0.0244141         0.0         0.0         0.0     1000.0          0.0       6.0  6.25E-04
   1     1     1     1     1     1   111     0 0000     0     0                 R2-13
   0     0     0     0     0     0     0     0    0     0                       R2-1
 0.0434028         0.0         0.0         0.0     1000.0          0.0       6.0  6.25E-04
   1     1     1     1     1     1   111     0 0000     0     0                 R2-13
   0     0     0     0     0     0     0     0    0     0                       R2-1
 0.0976563         0.0         0.0         0.0     1000.0          0.0       6.0  6.25E-04
   1     1     1     1     1     1   111     0 0000     0     0                 R2-13
   0     0     0     0     0     0     0     0    0     0                       R2-1
  0.390625         0.0         0.0         0.0     1000.0          0.0       6.0  6.25E-04
   1     1     0     1     1     1   111     0 0000     0    11                 R2-13
   0     0     0     0     0     0     0     0    0     0                       R2-1
   0.61035         0.0         0.0         0.0     1000.0          0.0       6.0  6.25E-04
   1     1     1     1     1     1   111     0 0000     0     0                 R2-13
   0     0     0     0     0     0     0     0    0     0                       R2-1
   1.08507         0.0         0.0         0.0     1000.0          0.0       6.0  6.25E-04
   1     1     1     1     1     1   111     0 0000     0     0                 R2-13
   0     0     0     0     0     0     0     0    0     0                       R2-1
  1.265625         0.0         0.0         0.0     1000.0          0.0       6.0  6.25E-04
   1     1     1     1     1     1   111     0 0000     0     0                 R2-13
   0     0     0     0     0     0     0     0    0     0                       R2-1
   1.97754         0.0         0.0         0.0     1000.0          0.0       6.0  6.25E-04
   1     1     1     1     1     1   111     0 0000     0     0                 R2-13
   0     0     0     0     0     0     0     0    0     0                       R2-1
   2.44141         0.0         0.0         0.0     1000.0          0.0       6.0  6.25E-04
   1     1     1     1     1     1   111     0 0000     0     0                 R2-13
   0     0     0     0     0     0     0     0    0     0                       R2-1
  3.515625         0.0         0.0         0.0     1000.0          0.0       6.0  6.25E-04
   1     1     1     1     1     1   111     0 0000     0     0                 R2-13
   0     0     0     0     0     0     0     0    0     0                       R2-1
```

Figure 5.2-3. Problem 8. Listing of SWIFT II Input Data (Continued)

```
7.910165        0.0         0.0         0.0      1000.0         0.0        6.0  6.25E-04
  1     1     1     1     1     1   111     0 0000     0     0                 R2-13
  0     0     0     0     0     0     0     0     0     0                     R2-1
9 76563         0.0         0.0         0.0      1000.0         0.0        6.0  6.25E-04
  1     1     1     1     1     1   111     0 0000     0     0                 R2-13
  0     0     0     0     0     0     0     0     0     0                     R2-1
31 6406         0.0         0.0         0.0      1000.0         0.0       25.0  6.25E-04
  1     1     1     1     1     1   111     0 0000     0    11                 R2-13
  0     0     0     1     0     0     0     0     0                           R2-1-STOP
```

Figure 5.2-3. Problem 8. Listing of SWIFT II Input Data (Continued)

is unity for each saturated grid block, but for the partially-saturated block representing the location of the free-water surface, it is

$$\bar{S} = \Delta h/\Delta z \qquad (5.2\text{-}3a)$$

where Δh is the saturated thickness. This can be shown to reduce the storage term used by SWIFT II from

$$\frac{\partial}{\partial t}(\phi\rho S) \text{ to } \phi\frac{\partial h}{\partial t} . \qquad (5.2\text{-}3b)$$

Results. Results for the numerical and analytical solutions are plotted in Figure 5.2-2. For the small times the numerically calculated free-water surface drops more rapidly than that of the analytical solution. Otherwise, the agreement is quite reasonable. Rather than using the grid-block saturations, as in Problem 7, the grid-block pressures are used directly to calculate the free-water surface.

The distance of interest,

$$x = 0.025 \text{ m} \qquad (5.2\text{-}4a)$$

is at the center of the block I = 3 (see table, "X-Direction Distance to Grid-Block Center" in the microfiche). From the "Pressure-at-Elevation" table for

$$t = 9.77 \times 10^{-2} \text{ s} \qquad (5.2\ 4b)$$

which gives

$$\xi = (\phi/2K_x t)^{1/2} x = 0.4 \qquad (5.2\text{-}4c)$$

note that

$$p(3,6) = -42.46 \text{ Pa} . \qquad (5.2\ 5a)$$

The unsaturated block thickness is then

$$\Delta h(3,6) = 0.0294 \text{ m} \quad . \tag{5.2 5b}$$

Because all of the block thicknesses are $\Delta z = 0.05$ m, the free-water surface is

$$h(x,t) = (15)(0.05) - 0.0294 = 0.721 \text{ m} \tag{5.2-6a}$$

which agrees with Figure 5.2-4. The dimensionless elevation scaled with the minimum elevation $\frac{h_o}{2} = 0.5$ m is

$$h(0.4)/(h_o/2) = 1.44 \tag{5.2-6b}$$

which also agrees with Figure 5.2-2.

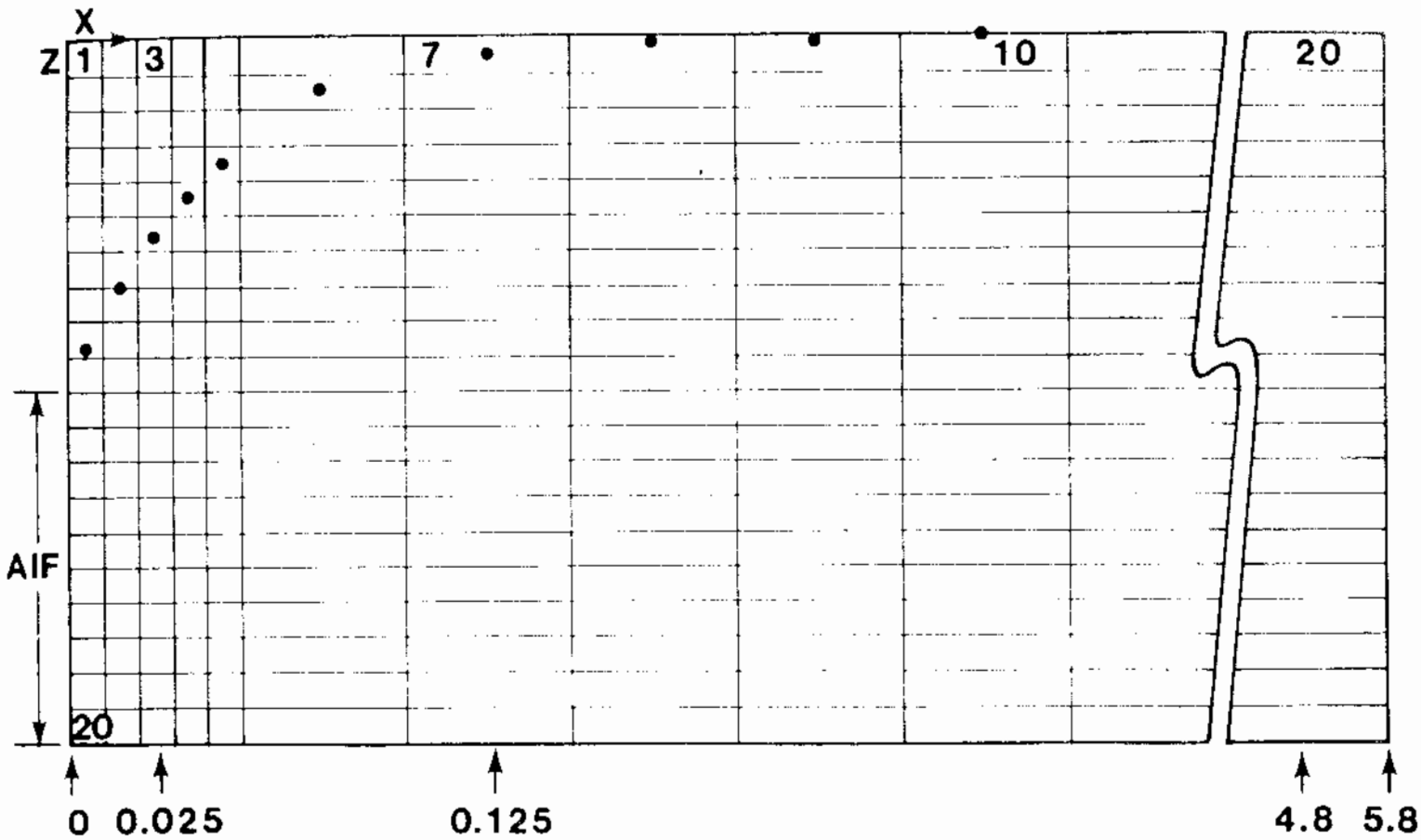

Figure 5.2-4. Gridding and Boundary Conditions (Labelled "AIF")

6. NOTATION*

ROMAN SYMBOLS

a	thickness of prism or radius of sphere for the local subsystem
a_W	explicit portion of e_W, the boundary flow rate of the simulated aquifer
A	radial grid block-ratio
A_V	global/local interface area specific to global volume
A_m	specific activity
b	aquifer thickness
b'	aquitard thickness
b_W	implicit portion of e_W, the boundary flow rate of the simulated aquifer
c_{pR}	specific heat of the rock
C_R	compressibility of the pores
c_w	compressibility of the fluid
C	concentration of radioactive (trace) components
d	fracture half-thickness
D	dispersion/diffusion
D_m	molecular diffusion in porous media
D^*	molecular diffusion in water
e_W	boundary flow rate into the simulated aquifer calculated using the Carter and Tracy (1960) method

---

* The terms "global" and "local" are used in this section. Typically, the global model is used to represent the fractures or the aquifer. It is regionally connected and may be three-dimensional. Usually, the local submodel is used to represent either the porous rock matrix or the confining beds; it is one-dimensional only.

g	acceleration of gravity
g_c	units conversion factor equal to g for the English system and equal to unity for the SI system
h	head
H	total head
I	radionuclide inventory
k_d	radionuclide distribution coefficient
K_v	dimensionless distribution coefficient, $K_v = \rho_R k_d$
K	retardation factor or hydraulic conductivity
L	length
m	density of radioactive waste, i.e., mass of radionuclide per volume of waste
n_s	number of nodes within a local unit
p	pressure
P_I	influence function used in the Carter Tracy (1960) method
Q	mass injection rate
q	mass source rate or fluid recharge rate
q_w	radionuclide source due to waste leaching
Q	rate of fluid withdrawal from well
r	radial coordinate
r_e	external radius of aquifer model
r_o	extent of assumed stress-relief fracturing
r_w	radius of wellbore
r_1	radius of skin or radius to center of first grid block
R_w	source term for release of nuclides from the waste matrix
s	one-dimensional coordinate for the local units

$\bar{s}$	drawdown
S	storativity
S_s	specific storativity
$\ddot{S}$	saturation
t	time
t_a	total leach time
t_D	dimensionless time
T	temperature, transmissivity or leach duration time
u	Darcy flux
U	mass flow rate through radionuclide inventory
v	interstitial velocity
WI	well index
x,y,z	Cartesian coordinates

GREEK SYMBOLS

α_L	longitudinal dispersivity
Γ	global-to-local radionuclide transfer rate
Γ_H	global-to-local heat transfer rate
Γ_W	global-to-local flow rate
δp	incremental change in pressure over a time step Δt
Δh	head increment
Δs	spatial increment in s for the local subsystem
Δt	time increment
Δx_i	spatial increment in x_i where $x_i = x$, $x_2 = y$, and $x_3 = z$
λ	decay constant

ξ	dimensionless Boltzmann variable
ρ	fluid density
ρ_R	formation density
ρ_w	volumetric waste density, i.e., volume of waste per bulk volume
τ	radionuclide half-life
τ	tortuosity
Φ	porosity

SUBSCRIPTS

m	fluid-plus-rock composite material
r	component number in a chain of species
w	radionuclide source (repository)
x,y,z	directional indicator

SUPERSCRIPTS

'	denotes local subsystem
~	indicates characteristic length

REFERENCES

Avdonin, N. A., 1964. Some Formulas for Calculating the Temperature Field of a Stratum Subject to Thermal Injection, Neft' i Gaz, Vol. 7, No. 3, pp. 37-41.

Bear, J., 1972. Dynamics of Fluids in Porous Media, American Elsevier Publishing Co., New York.

Carter, R. D., and Tracy, C. W., 1960. An Improved Method for Calculating Water Influx, Trans. SPE of AIME, 219, pp. 415-417.

Dennehy, K. F. and Davis, P. A., 1981. Hydrologic Testing of Tight Zones in Southeastern New Mexico, Ground Water, Vol. 19, No. 5, pp. 482-489.

Dillon, R. T., Lantz, R. B., and Pahwa, S. B., 1978. Risk Methodology for Geologic Disposal of Radioactive Waste: The Sandia Waste-Isolation Flow and Transport (SWIFT) Model, NUREG/CR-0424 and SAND78 1267, Sandia National Laboratories, Albuquerque, New Mexico.

Finley, N. C., and Reeves, M., 1981. SWIFT Self Teaching Curriculum: Illustrative Problems to Supplement the User's Manual for the Sandia Waste-Isolation Flow and Transport Model (SWIFT), NUREG/CR-1968 and SAND81-0410, Sandia National Laboratories, Albuquerque, New Mexico.

Hantush, M. S., 1960. Modification of the Theory of Leaky Aquifers, J. Geophys. Res., Vol. 65, pp. 3713-3725.

Huyakorn, P. S., 1983. FTRANS, A Two-Dimensional Code for Simulating Fluid Flow and Transport of Radioactive Nuclides in Fractured Rock for Repository Performance Assessment, ONWI-426, Battelle Memorial Institute, Office of Nuclear Waste Isolation, Columbus, Ohio.

INTERCOMP Resource Development and Engineering, Inc., 1976. Development of Model for Calculating Disposal in Deep Saline Aquifers, Parts I and II, USGS/WRI-76-61, PB-256903, National Technical Information Service, Washington, D.C.

INTRACOIN, 1983. International Nuclide Transport Code Intercomparison Study, Swedish Nuclear Power Inspectorate, Stockholm, Sweden.

Mercer, J. W., and Orr, B. R., 1979. Interim Data Report on the Geohydrology at the Proposed Waste Isolation Pilot Plant Site in Southeast New Mexico, U.S. Geo. Survey, Water Resour. Inv. 79-98.

Pahwa, S. B., and Baxley, P. T., 1980. Detection of Fractures from Well Testing in Proceedings: Workshop on Numerical Modeling of Thermohydrological Flow in Fractured Rock Masses, LBL-11566 and ONWI-240, Battelle Memorial Institute, Office of Nuclear Waste Isolation, Columbus, Ohio.

Powers, D. W., Lamber, S. J., Shaffer, S., Hill, L. R., and Weart, W. D., 1978. Geological Characterization Report, Waste Isolation Pilot Plant (WIPP) Site, Southeast New Mexico, Vols. I and II, SAND78-1596, Sandia National Laboratories, Albuquerque, New Mexico.

Rasmuson, A., 1984. Migration of Radionuclides in Fissured Rock: Analytical Solutions for the Case of Constant Source Strength, Water Resour. Res., Vol. 20, No. 10, pp. 1435 - 1442.

Reeves, M., and Cranwell, R. M., 1981. User's Manual for the Sandia Waste-Isolation Flow and Transport Model (SWIFT) Release 4.81, NUREG/CR-2324 and SAND81-2516, Sandia National Laboratories, Albuquerque, New Mexico.

Reeves, M., Ward, D. S., Johns, N. D., and Cranwell, R. M., 1986a. Theory and Implementation for SWIFT II, The Sandia Waste-Isolation Flow and Transport Model for Fractured Media, NUREG/CR-3328 and SAND83-1159, Sandia National Laboratories, Albuquerque, New Mexico.

Reeves, M., Johns, N. D., and Cranwell, R. M., 1986b. Data Input Guide for SWIFT II, The Sandia Waste-Isolation Flow and Transport Model for Fractured Media, NUREG/CR-3162 and SAND83-0242, Sandia National Laboratories, Albuquerque, New Mexico.

Ross, B., Mercer, J. W., Thomas, S. D., and Lester, B. H., 1982. Benchmark Problems for Repository Siting Models, NUREG/CR-3097, U.S. Nuclear Regulatory Commission, 138 pp.

Tang, D. H., Frind, E. O., and Sudicky, E. A., 1981. Contaminant Transport in Fractured Porous Media: 1. Analytical Solution for a Single Fracture, Water Resour. Res., Vol. 17, No. 3, pp. 555-564.

Ward, D. S., Reeves, M., and Duda, L. E., 1984a. Verification and Field Comparison of the Sandia Waste-Isolation Flow and Transport Model (SWIFT), NUREG/CR-3316 and SAND83-1154, Sandia National Laboratories, Albuquerque, New Mexico.

Ward, D. S., Reeves, M., Huyakorn, P. H., Lester, B., Ross, B., and Vogt, D., 1984b. Benchmarking of Flow and Transport Codes for Licensing Assistance, GeoTrans, Inc. and Teknekron, Inc., to be published as a NUREG report.